FINAL REPORT FOR ELECTROCHEMICAL CELLS FOR USE IN A BALLOON ENVIRONMENT

Contract No.: NAS5-11548

Prepared by

MELPAR, INC.
7700 Arlington Boulevard
Falls Church, Virginia 22046

for

GODDARD SPACE FLIGHT CENTER
Greenbelt, Maryland

Final Report

for

ELECTROCHEMICAL CELLS FOR USE IN A BALLOON ENVIRONMENT

Contract No.: NAS5-11548

Prepared by

Melpar, Inc.
7700 Arlington Boulevard
Falls Church, Virginia 22046

for

Goddard Space Flight Center
Greenbelt, Maryland

TABLE OF CONTENTS

LIST OF ILLUSTRATIONS

LIST OF TABLES

1. INTRODUCTION

The objective of this program was to fabricate, test and characterize Ag/Zn electrochemical cells with a solid electrolyte* for potential use in a balloon environment.

The cells were tested at 25°C and 0°C and exhibited an open circuit voltage from 0.9 to 0.98 volts, a maximum current density of 25 ma/cm^2 at 25°C, and were capable of being recharged. For operation to 25% depth of discharge at 0°C, the maximum current density was 132 μa/cm^2 with 21 recharges, or 310 μa/cm^2 with 6 recharges.

Although the number of cycles is far below that of 180 required for the balloon battery program, the present Ag/Zn electrochemical system studied has shown promise in this initial investigation and is the first rechargeable solid electrolyte cell reported.

Complete fabrication methods, structural details, test equipment and representative cell performance data are reported as well as recommendations for future development.

---

*Basic research leading to the establishment of the solid electrolyte composition and cell fabrication methods were carried out under Melpar Inc.'s Independent Research and Development Program. Patent protection for the basic aspects of the cell reported herein is being sought.

2. STRUCTURE AND FABRICATION OF Ag-Zn SOLID ELECTROLYTE BATTERY

2.1. Structure of Cell

The electrochemical cell studied under this contract had the following structure:

$$Ag/AgCl/\ \genfrac{}{}{0pt}{}{ZnCl_2}{LiCl} \cdot 2NH_3 \cdot H_2O/Zn\ (Hg)$$

The theoretical energy density and related data are given in Table 1.

Based on the assumed reversible reaction:

$$AgCl + 1/2\ Zn + NH_3 + 1/2\ H_2O \rightleftharpoons Ag + 1/2\ (ZnCl_2 \cdot 2NH_3 \cdot H_2O)$$

the theoretical energy density can be calculated:

$$Ag = 4.03\ g/Ah + 1/2\ ZnCl_2 \cdot 2NH_3 \cdot H_2O = 3.51\ g/Ah = 7.54\ g/Ah = 60\ Ah/lb.$$

Based on the EMF of 0.85 to .95 volts, the corresponding density is 51 to 57 watt hours per pound of active material. It should then be recognized that the reaction assumed above has not been confirmed and is probably only approximately correct. When the cells are assembled in the charged state, there is no source of NH_3 and probably no source of H_2O as required for stoichiometric balance. Without a determination of the cell components in the charged and discharged states, reaction (s) occurring are unknown. This high energy density of 60 watt hours/lbs. is one principal advantage of this system for power supplies for weather balloon data acquisition systems.

TABLE 1

Theoretical Values and Related Data of the Cell

	Ag	AgCl	1/2 $ZnCl_2$	1/2 $(ZnCl_2 \cdot 2NH_3 \cdot H_2O)$	1/2 Zn
Mol Weight	107.88	143.34	68.15	94.19	32.7
Gram/Ah	4.025	5.36	2.54	3.51	1.22
Density gram/cm^3	10.5	5.56	2.91	2.10	7.14
cm^3/Ah	0.384	0.965	0.875	1.67	0.171
Thickness (μ) for one mAh/cm^2	0.384	9.65	8.75	16.7	1.71
Thickness (μ) for 25 mAh cell with 6.45 cm^2 area	14.88	37.39	33.91	64.7	6.63

The $Zn/ZnCl_2 \cdot 2NH_3$ half cell has a potential of 0.768 volts at 25°C and that of Ag/AgCl a potential of 0.22 volts, yielding a potential of almost 1 volt for the cell. The highest potential observed was 0.98 volts for a few cells immediately after they were fabricated.

2.2. Fabrication of Ag-Zn Cells

2.2.1. Preparation of Ag/AgCl half cell

A sheet of 1.5 mil Ag was cut into electrodes as shown in Figure 1. The Ag was cleaned with benzene in an ultrasonic cleaning unit followed by rinses of acetone, distilled water, and grain alcohol. The Ag electrode was then held rigid by a back support of Scotch dielectric tape #470 and masked with the tape on the reverse side to expose an area of 6.45 cm^2 (1-1/8" diameter). Six such electrodes were then placed in a dilute HCl (approximately 0.2N) bath and approximately 15μ of silver were converted to 37μ of AgCl by electrolysis at a rate of 3.88 mA/cm^2, thus producing a 25 mAh cell capacity. The Ag/AgCl half cell was then left in distilled water for several hours and dried.

2.2.2. Preparation of the Zn Electrode

A sheet of 2 mil Zn was cut and cleaned by the same method as the Ag. In addition, however, the Zn was amalgamated by rubbing it with a 10% solution of $HgCl_2$. Dielectric tape was used to make the cell rigid and to assist in

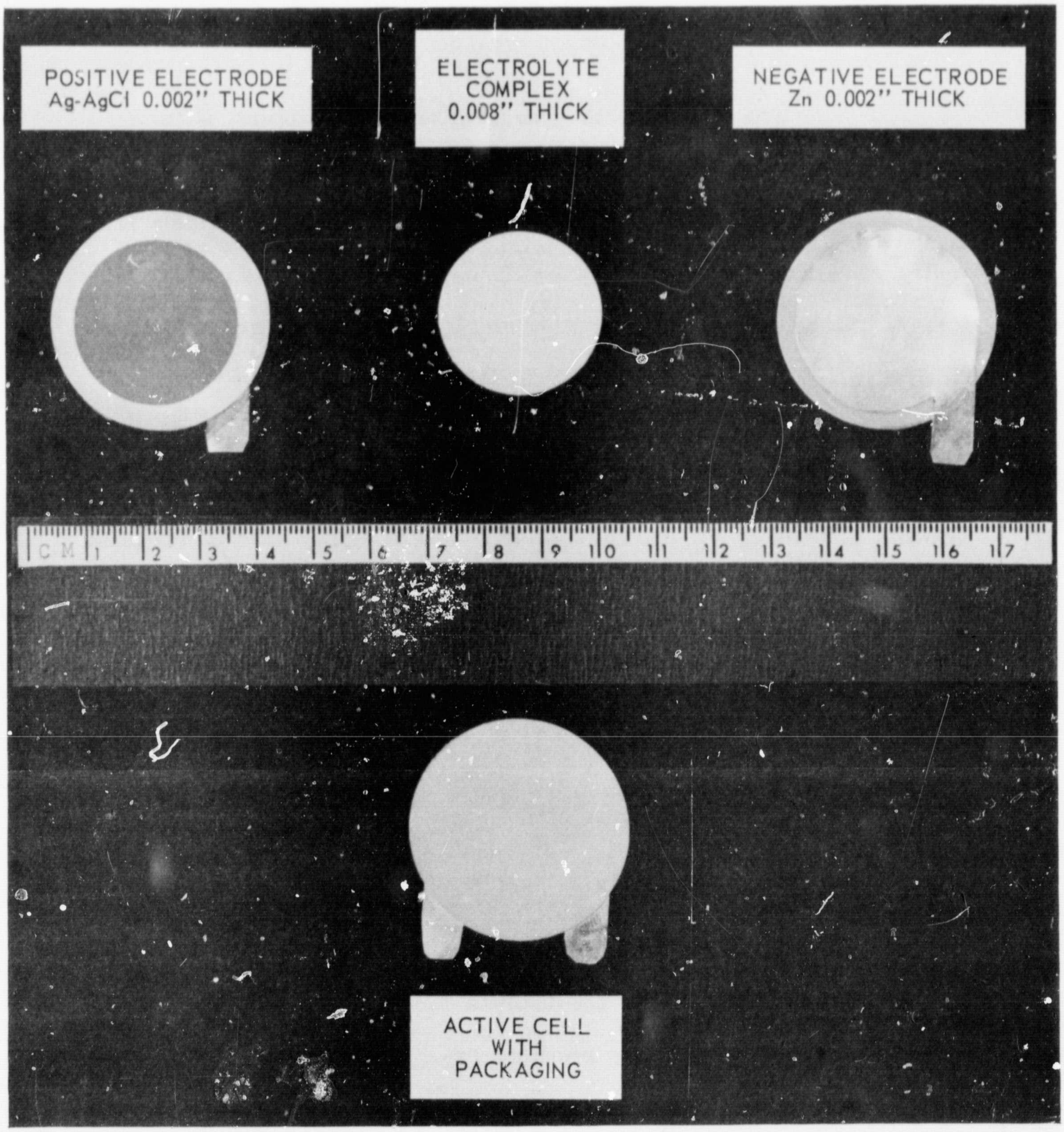

Figure 1. Structure of Solid Electrolyte Cell

sealing the cell as shown in Figure 1.

2.2.3. Preparation of the Electrolyte

The electrolyte was prepared by dipping filter paper, 100μ thick, into a $ZnCl_2$ + LiCl solution (100 g of $ZnCl_2$, 4g LiCl, 50 ml H_2O). This was then exposed for 72 hours to ammonia gas while being dried in a desiccator containing "Dririte" ($CaSO_4$). The ammine complex formed after this step had a very high resistance. After exposure to 93% relative humidity for 1.5 to 2 hours, the AC resistance dropped to less than 10 ohm. Careful weighing of the electrolyte showed a gain of 10.6% in weight corresponding to the addition of 1 molecule of water.

$$ZnCl_2 \cdot 2NH_3 + H_2O \longrightarrow ZnCl_2 \cdot 2NH_3 \cdot H_2O$$

$$170.3 + 18 \longrightarrow 188.3 \quad \text{or} \quad \frac{18}{170.3} = 10.6\%$$

calculated gain in weight

2.2.4. Cell Assembly

The cell was completed by using one or two layers of the fibrous paper with electrolyte between the Ag/AgCl and Zn(Hg) electrodes. Next, another layer of dielectric tape was applied over each electrode to provide a greater mositure barrier and the entire cell dipped in a krylon solution.

3. GENERAL CELL CHARACTERISTICS

Immediately after the cell was fabricated, dipped and dried, the open circuit voltage, E_o, and the AC resistance were measured.

E_o ranged from 0.9 to 0.98 volts and the AC resistance from 4 to 10 ohms. The DC internal resistance was calculated by the following formula:

$$R = \frac{V_2 - V_1}{I_2 - I_1}$$

where $V_1 = V_L$ when $I_1 = 500\mu A$

or $V_2 = V_L$ when $I_2 = 1000\mu A$

The variation of the cell resistance with temperature was determined for numerous cells, Figure 2 being a typical example. The internal resistance decreased on the 2nd discharge, probably because of an increase in surface contact between the various cell layers. The resulting resistivity of the solid electrolyte is on the order of 300 ohm - cm.

The variation of cell voltage with temperature can be calculated from the thermodynamics of the reaction by the equation:

$$\frac{(dE)}{(dT)_p} = \frac{\Delta s}{23060j}$$

where j = 1 in this case and Δs is the change in entropy. Using the value of 4.78 E.U. for Δs, the temperature coefficient was

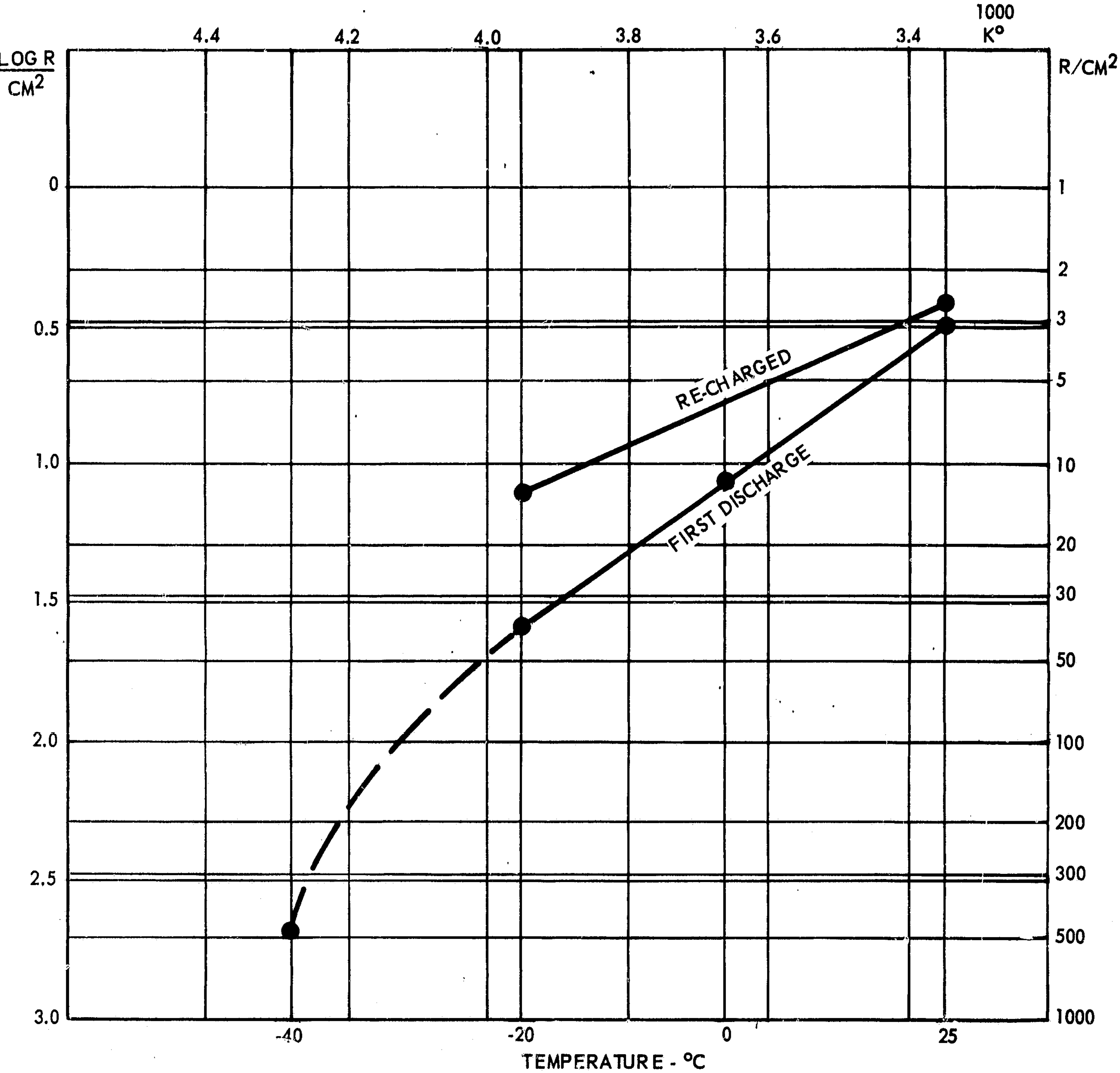

Figure 2. Variation of Cell Resistance with Temperature

calculated to be 0.2 mv/°K and is therefore no greater than 5 mv for a 25°K temperature change.

As stated above, the theoretical capacity of the cell, (25 mAh), is limited by the thickness of the AgCl. (At 25°C the actual capacity at a discharge rate of 125 $\mu A/cm^2$ was found to be 60% of the theoretical, or 15 mAh, as shown in Figure 3. The actual capacity was defined as the cell capacity when E_L dropped to 0.72 volts, or approximately 80% E_o.) This value was used in characterizing the double layer cells which provided most of the data reported.

The maximum current density at 25°C of all cells fabricated was approximately 25 mA/cm^2, as shown in Figure 4, when the voltage dropped to the lower limit of 0.72 volts.

4. TEST EQUIPMENT

Each battery cell was placed under pressure by a special clamp, as shown in Figure 5, and the screw tightened by a torque screwdriver. This prevented separation of the cell layers and assured proper contact. The cycling control circuits utilized for determining the battery performance are shown in Figures 6 and 7. There were four banks with five circuits in each, or a total of 20 circuits. Each circuit permitted charge and discharge at a constant current from 0 to 10 mA. In addition, a voltage limit could be set for both charge and discharge, and the current limited as shown in Figure 8. Each

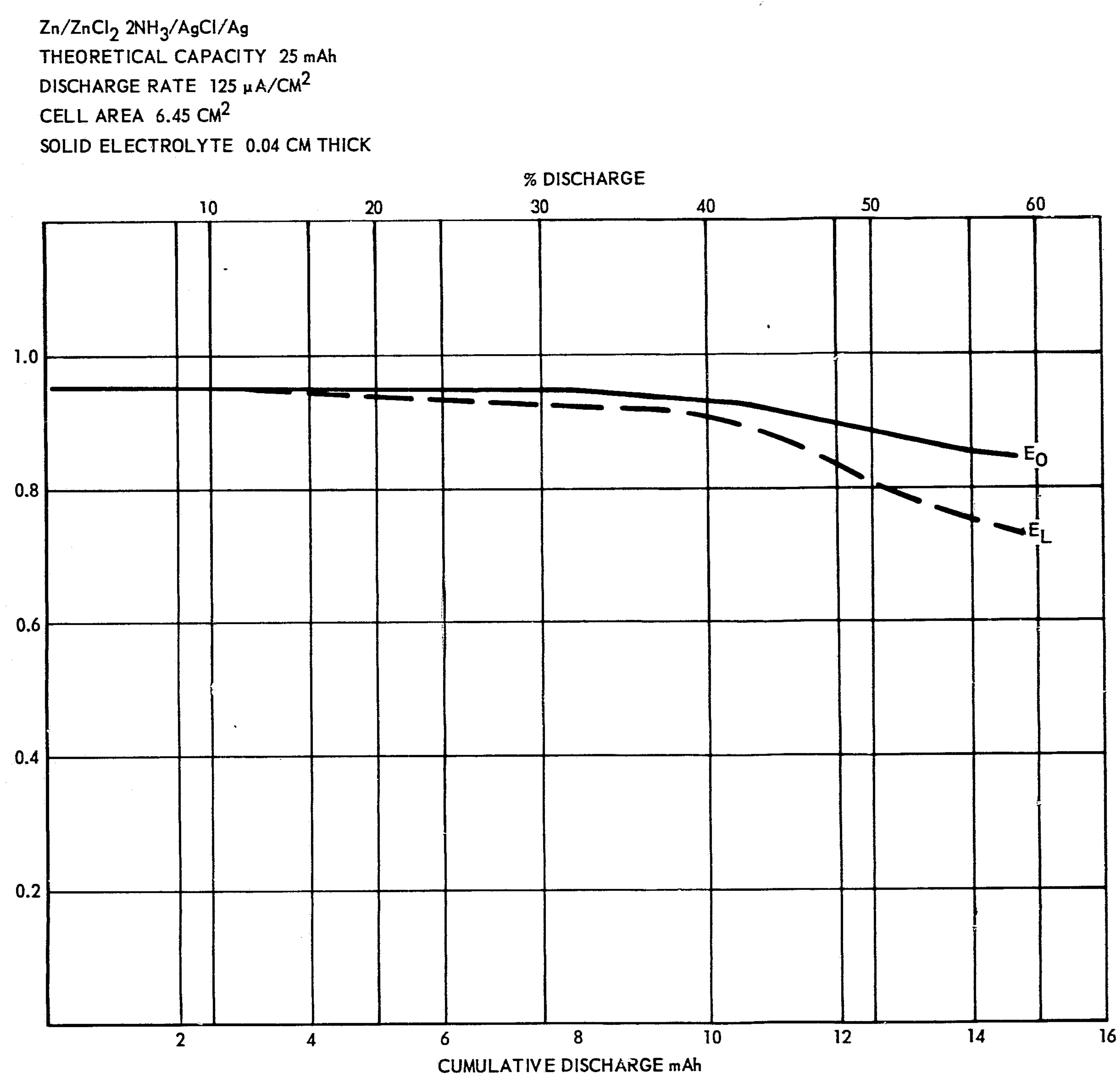

Figure 3. Cell Capacity at 25°C

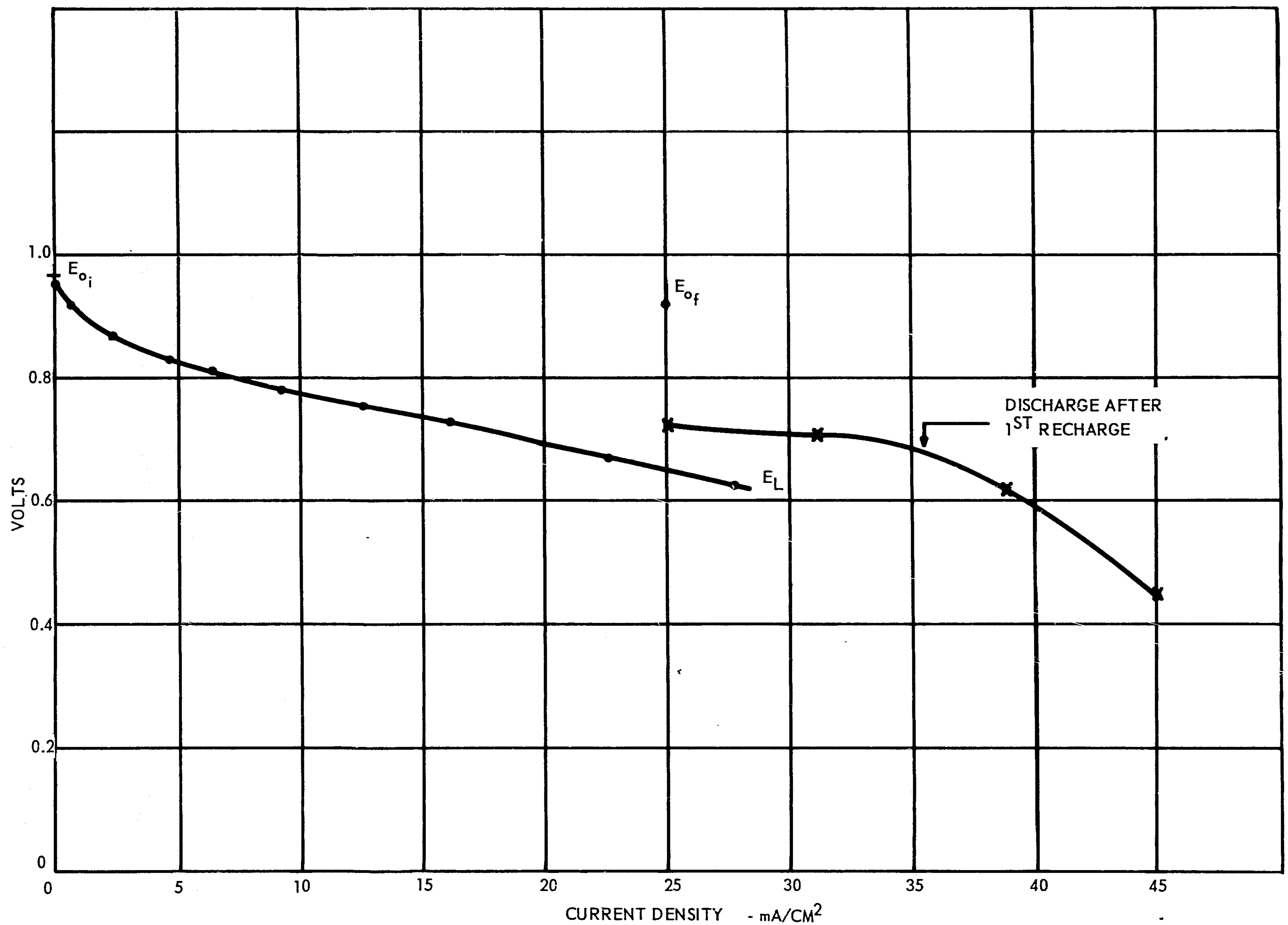

Figure 4. Maximum Current Density at 25°C

B0323

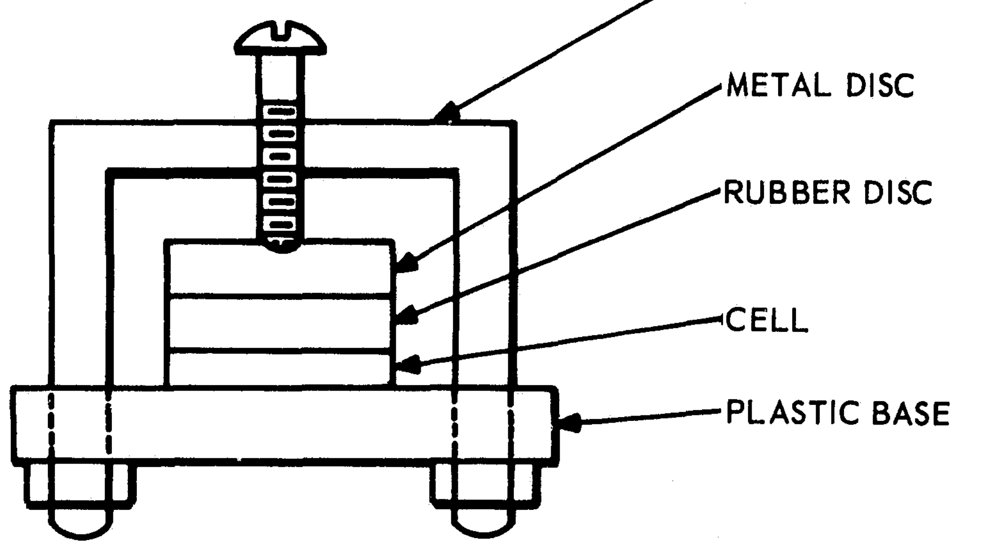

Figure 5. Pressure Clamp Used for Cell Testing

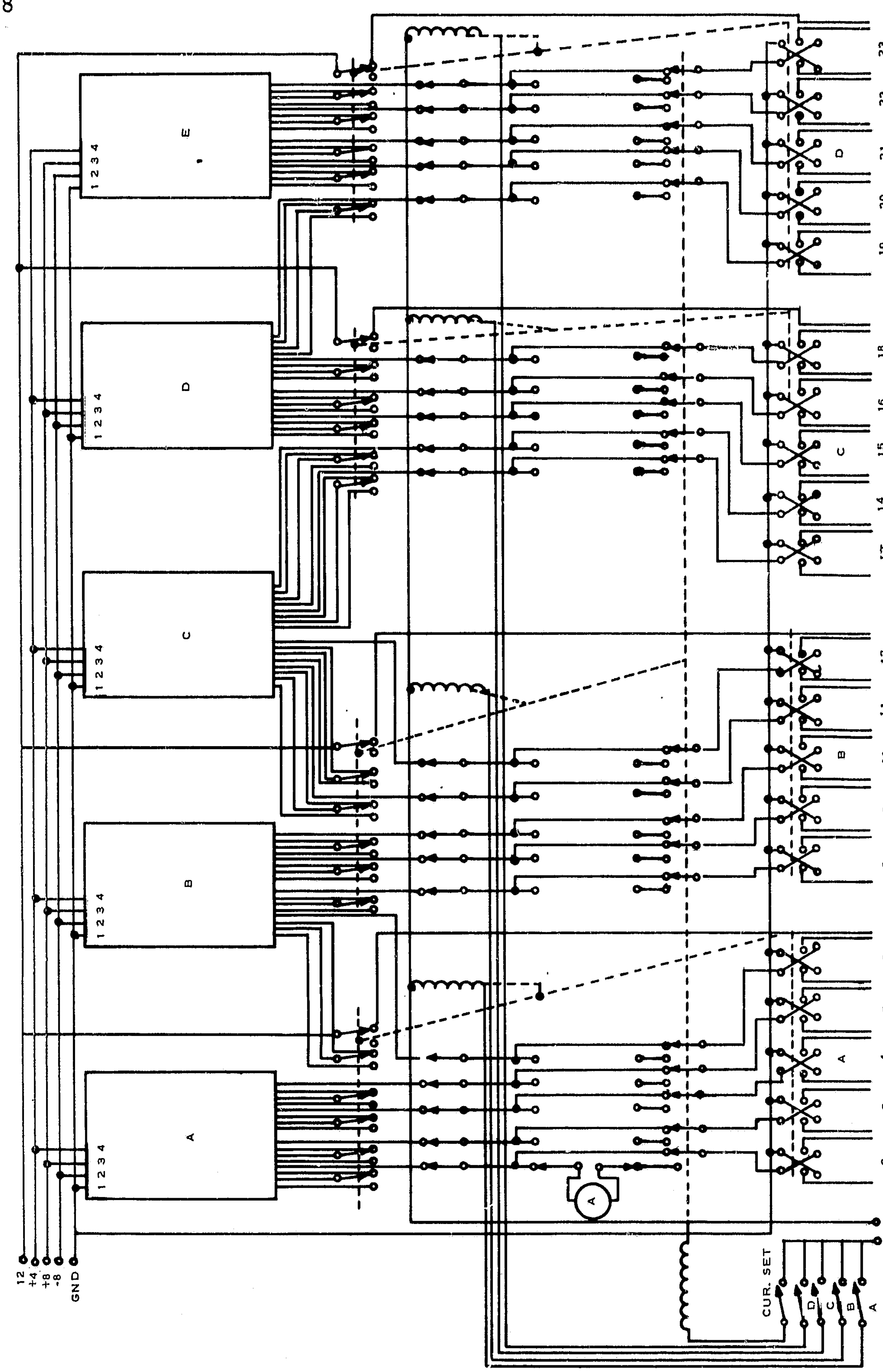

Figure 6. Diagram of Battery Control Circuits

B0189

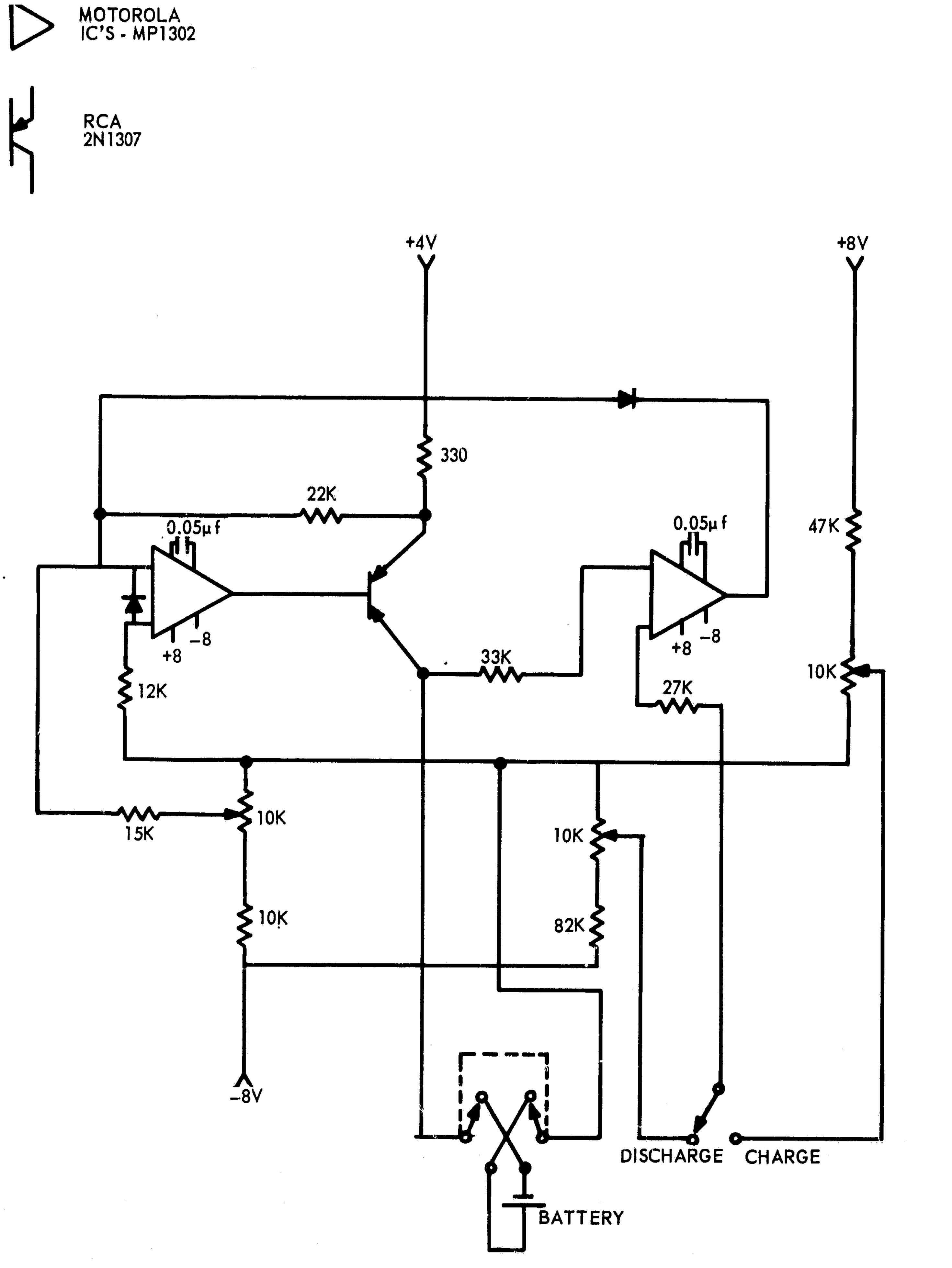

Figure 7. Circuit for Discharging and Charging Batteries at Constant Current and for Limiting the Current for Preset Discharge and Charge Voltages

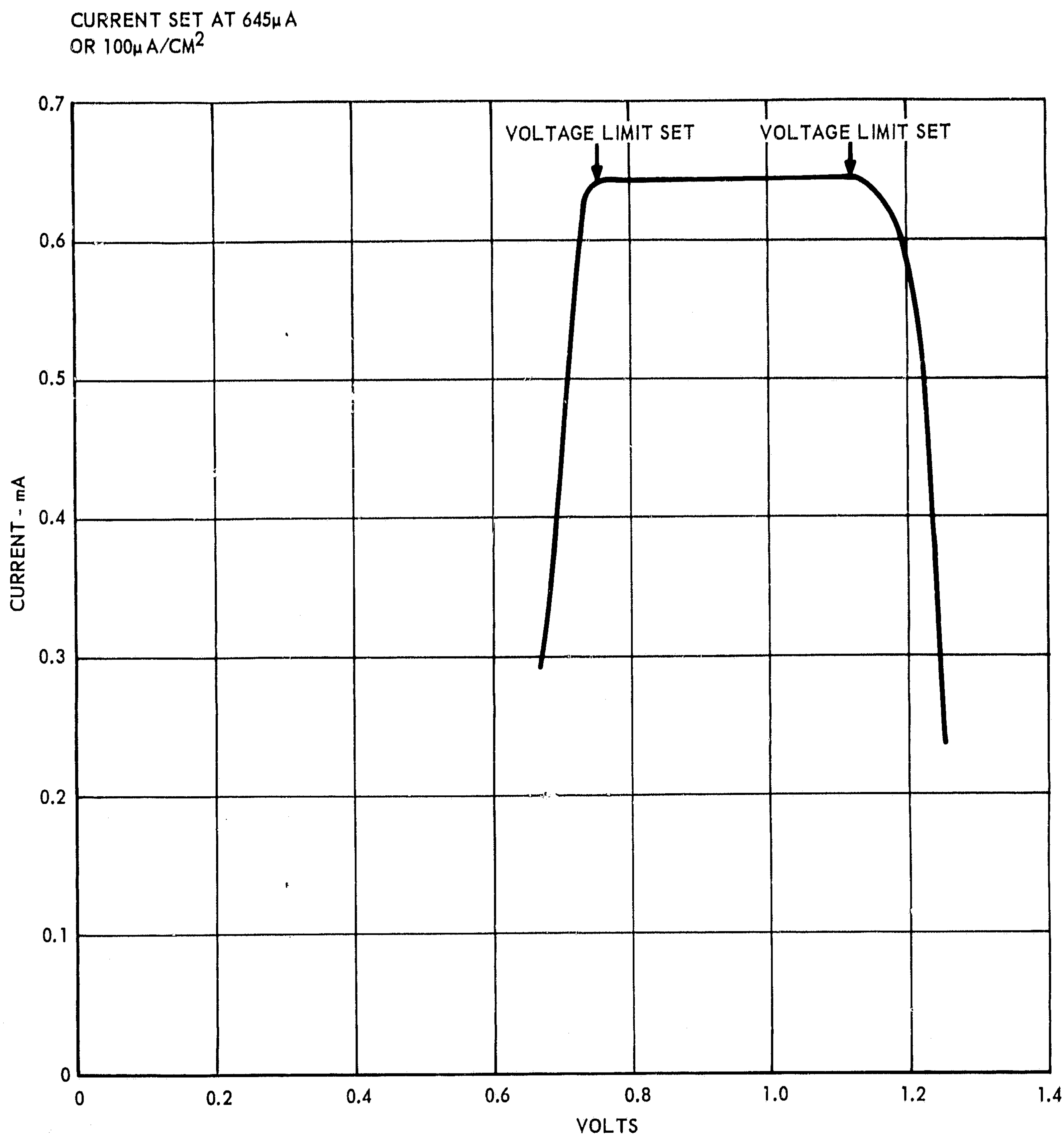

Figure 8. Example of the Current Limiting for a Preset Charge and Discharge Voltage Limit

bank of batteries, or groups of banks, was controlled by a separate 24-hour timing switch to permit a variety of charge, discharge cycles. Three 0-50V Power Design power supplies were used for the +4, +8 and -8 volts. The operational amplifiers were integrated circuits Motorola type MP1302 and the transistors RCA type 2N1307 which have a β of 60 or greater at 10 ma.

The cell voltage was recorded periodically by the test equipment arrangement shown in Figure 9. A programable stepping relay with a motor drive permitted a timed selection of each cell on tests and a print-out of the cell voltage.

5. CELL POLARIZATION

The solid electrolyte cell studied showed detectable polarization for discharge currents above 800-1,000 μA per the cell or 125 -155 $\mu A/cm^2$. In order to determine the relative contribution of the two electrodes, a standard cell was fabricated with a reference electrode of Ag/AgCl between the double layer of the electrolyte. The voltage was then measured from the reference electrode to each of the electrodes as the cell was discharged. The results are shown in Figure 10. At a discharge rate of 1,000 $\mu A/cm^2$, the polarization on the Ag/AgCl anode was near 0.1 volt and on the Zn cathode only about 0.03 volts. Polarization studies of the Ag electrode by Takahashi and Yamamoto revealed a reaction polarization

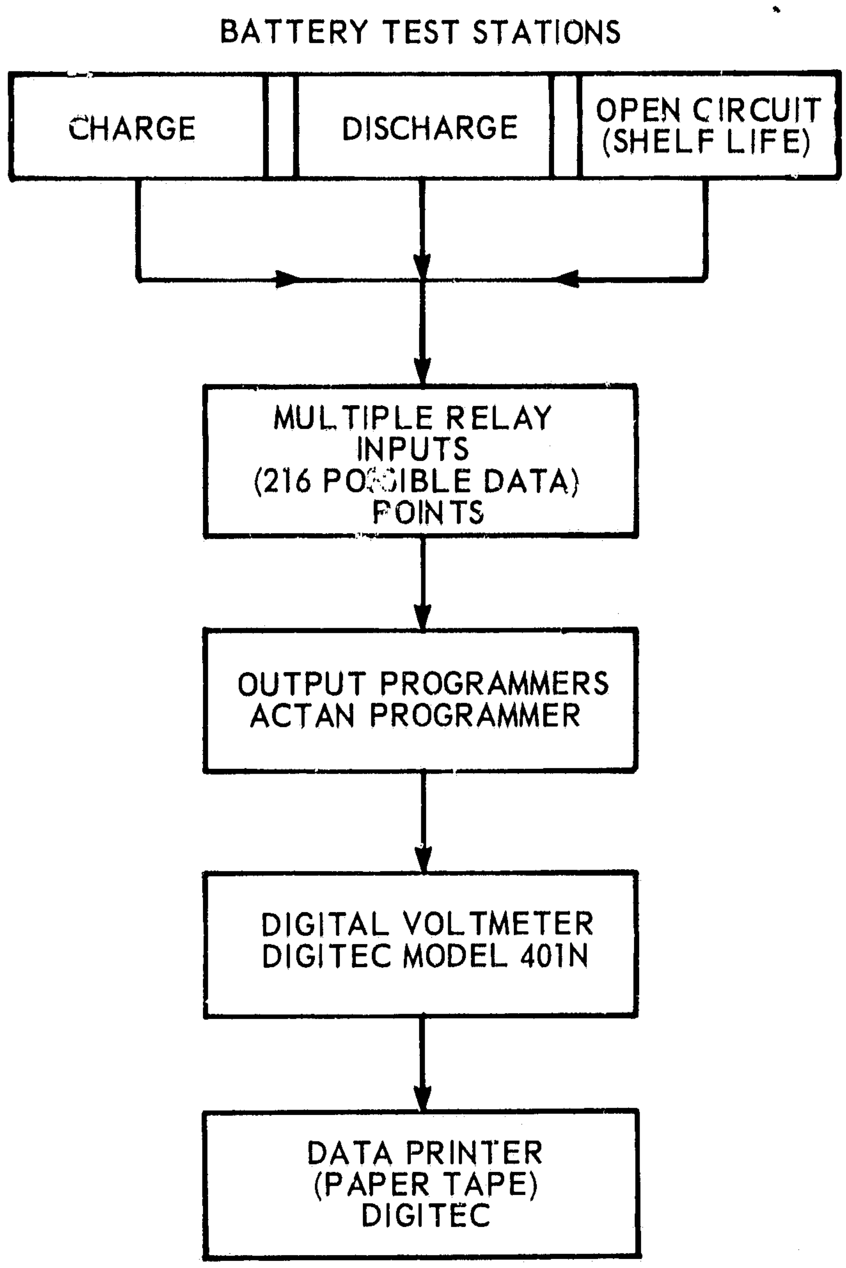

Figure 9. Block Diagram of the Voltage Sampling Circuit

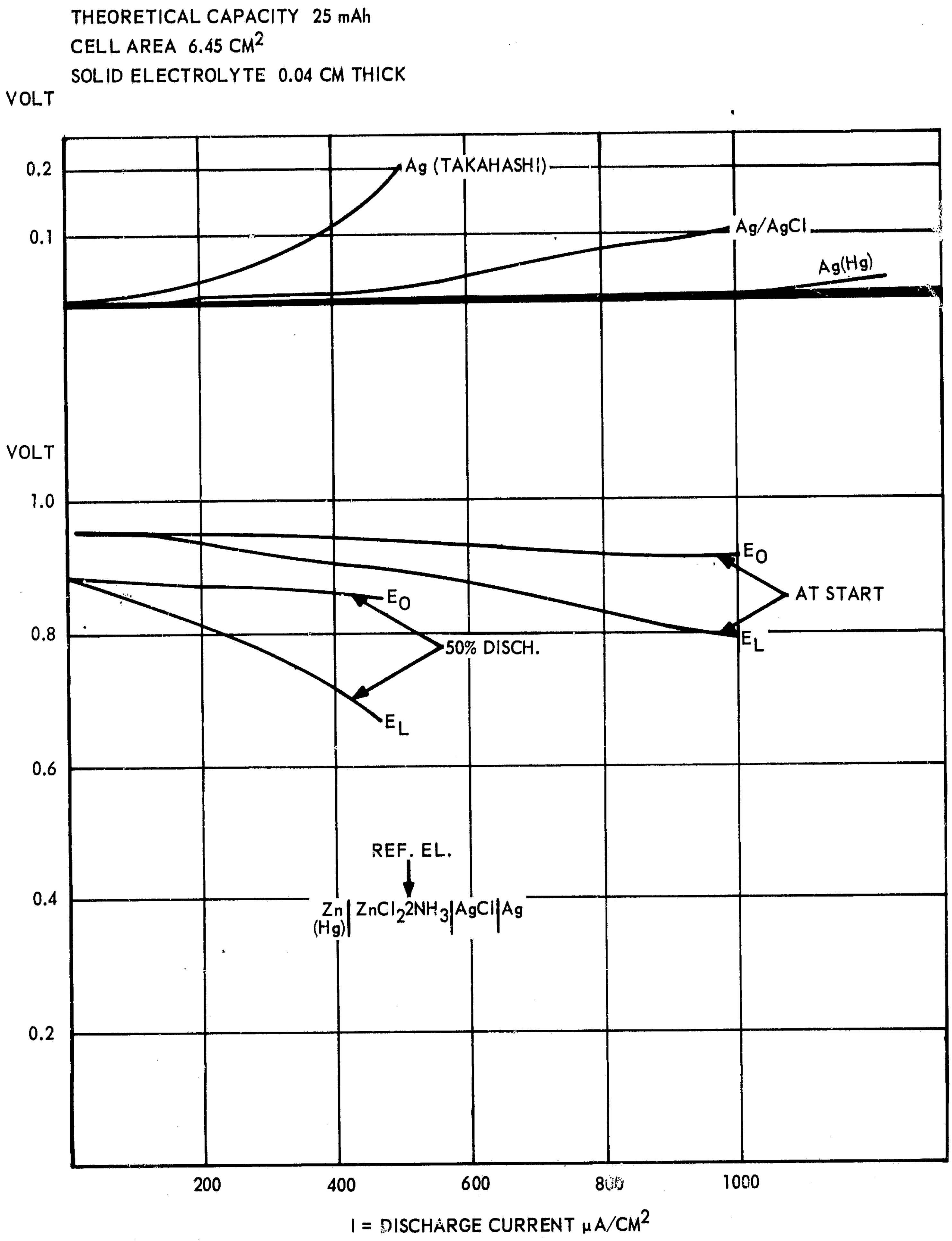

Figure 10. Discharge of Cell with Reference Electrode Showing the Amount of Ag/AgCl Polorization

mechanism in the solid electrolyte cell of $Ag/Ag_3SI/I_2$.* The mechanism was the reaction of an interstitial silver ion with a silver-ion vacancy. If the silver is amalgamated, this polarization is greatly reduced as their results shown in Figure 10. Their results are shown for comparison with our Ag/AgCl cell and suggest that amalgamation may be expected to reduce the polarization of the Ag-Zn cell considerably.

6. PERFORMANCE OF THE CELLS

6.1. Results at 25°C

The cells designated series 48 were used to characterize the performance of the electrochemical system. Series 48 cells employed two layers of 100μ thick filter paper no. 50 made by W & R Balston, Ltd. It should be pointed out that the size and thickness of the electrodes and the fibrous membrane were chosen strictly for convenience and no attempt was made to minimize weight or total cell thickness.

The first tests were made at room temperature (25°C) with no overcharge, i.e., the exact number of mAh discharged were replaced during charge. The results of these tests are summarized in Table 2. For this series per cent discharge is given as the per cent of the theoretical capacity which was 25 mAh.

---

*T. Takahaski and O. Yamamoto, "Polarization of the Solid Electrolyte Cell $Ag/Ag_3SI/I_2$", Electrochemica Acta, 1966 Vol. II, 01 911-917.

TABLE 2

Cycling Results at 25°C Without Overcharge

Cell No.	Eo_i volts	I μA	I/Area $\mu A/cm^2$	Discharge mAh	Discharge %TC	No. of Cycles	R_{DC} Initial	R_{DC} Final
48-2	0.945	400	62	5.2	20	1	5	26
48-3	0.920	400	62	2.1	8.5	1/2	3	S
48-4	0.923	400	62	7	28	1	2	S
48-5	0.933	400	62	4.7	19	1/2	3	70
48-7	0.930	400	62	4.3	17	1-1/2	5	52
48-9	0.920	400	62	3.8	15	1	40	670
48-16	0.968	650	100	-	-	1/2	3	S
48-17	0.976	650	100	-	-	1/2	10	S
48-18	0.976	650	100	5.6	22	1/2	4	S
*58-20	0.852	650	100	5.6	22	1/2	74	S
*58-22	0.948	650	100	-	-	1/2	15	S
*58-23	0.952	650	100	-	-	1/2	19	S
*58-52	0.937	650	100	-	-	1/2	35	S
*58-53	0.937	650	100	-	-	1/2	48	S
*58-54	0.938	650	100	-	-	1/2	23	S
48-55	0.938	485	75	10	40	6	25	45
48-56	0.968	650	100	5.2	20	1/2	12	S
48-57	0.953	485	75	10	40	1st	40	20
	0.953	485	75	8	32	2nd	27	24
	0.950	325	50	6.5	25	3rd	3	-
48-59	0.928	485	75	10	40	1st, 3rd	11	92
		400	62	6.4	27	4th	-	-
48-62	0.932	625	97	3.75	25 AC	3		
48-63	0.934	625	97	3.75	25	4		
48-64	0.930	625	97	3.75	25	3		
48-65	0.934	625	97	3.75	25	8		
48-66	0.930	625	97	3.75	25	8		
48-68	0.926	625	97	3.75	25	13		
48-74	0.900	625	97	3.75	25	9		
48-75	0.904	625	97	3.75	25	9		
48-76	0.900	625	97	3.75	25	9		
48-77	0.898	450	70	2.70	18	13		
		500	78	3.00	20	3		
48-80	0.912	475	74	2.80	20	14		
48-81	0.908	450	70	2.70	18	14		
48-67	0.892	450	70	2.70	18	10		

*Fibrous membrane was bibulous paper
S -- Cell shorted internally
R_{DC} -- DC Resistance
TC -- Theoretical Capacity (25 mAh)
AC -- Actual Capacity

The cell emf listed is that measured before the first discharge or the initial value. Cells 58-20 to 58-54 were made with a bibulous paper and all shorted after the first discharge. Numerous other cells were made but are not reported here because they do not add to the analysis of the cell performance. Typical cell performance is illustrated by Figures 11-15. Figures 11 and 12 are the results for the current range 62-80 $\mu A/cm^2$ and Figures 13-15 for the current range 93-100 $\mu A/cm^2$. After cell no. 48-59 the maximum number of cycles observed was 14 for the lower current range and 13 for the higher range with averages of 11 and 7.5 respectively as shown in Figure 16. The cells of Figures 11-15 represent three discharge depths summarized as follows:

Cell No.	I/cm^2	%DD	No. of cycles
48-80	80	19	14
48-65	97-100	25	8
66	97-100	25	8
68	93-100	25	13
48-55	62-75	40	6*

Several of the cells failed by internal shorting and the remainder by increased internal resistance until V_L reached 0.72 volts.

6.2. Results at 0° C

One of the principal objectives of the program was the determination of the cell performance, including

25°C
CELL 48-55
62-75μ A/CM^2 FOR 21 HRS.
OR 66% DD (ACTUAL CAPACITY)
OR 40% DD (THEORETICAL CAPACITY)
AND NO OVERCHARGE

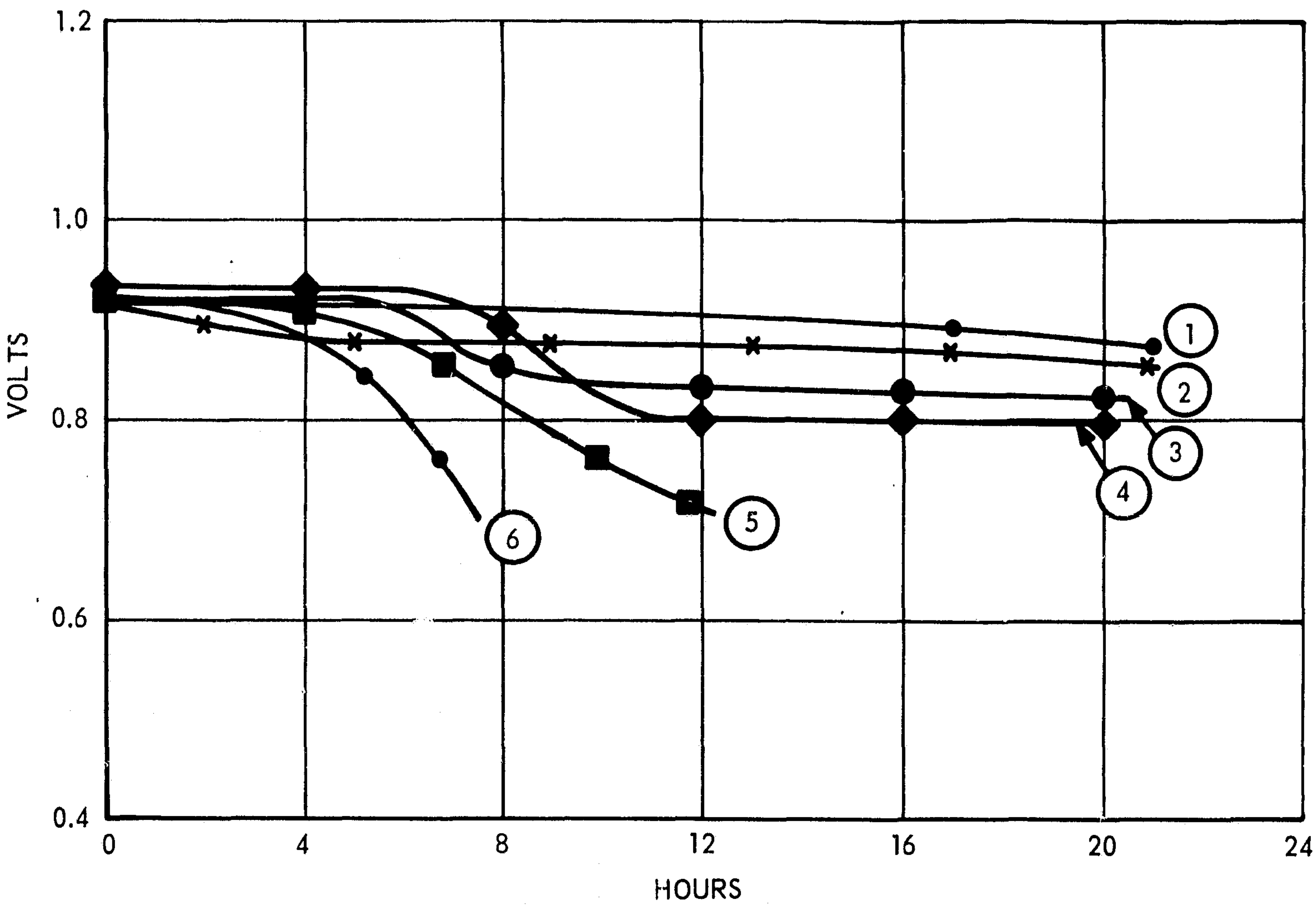

Figure 11. Performance Curves for Cell No. 48-55

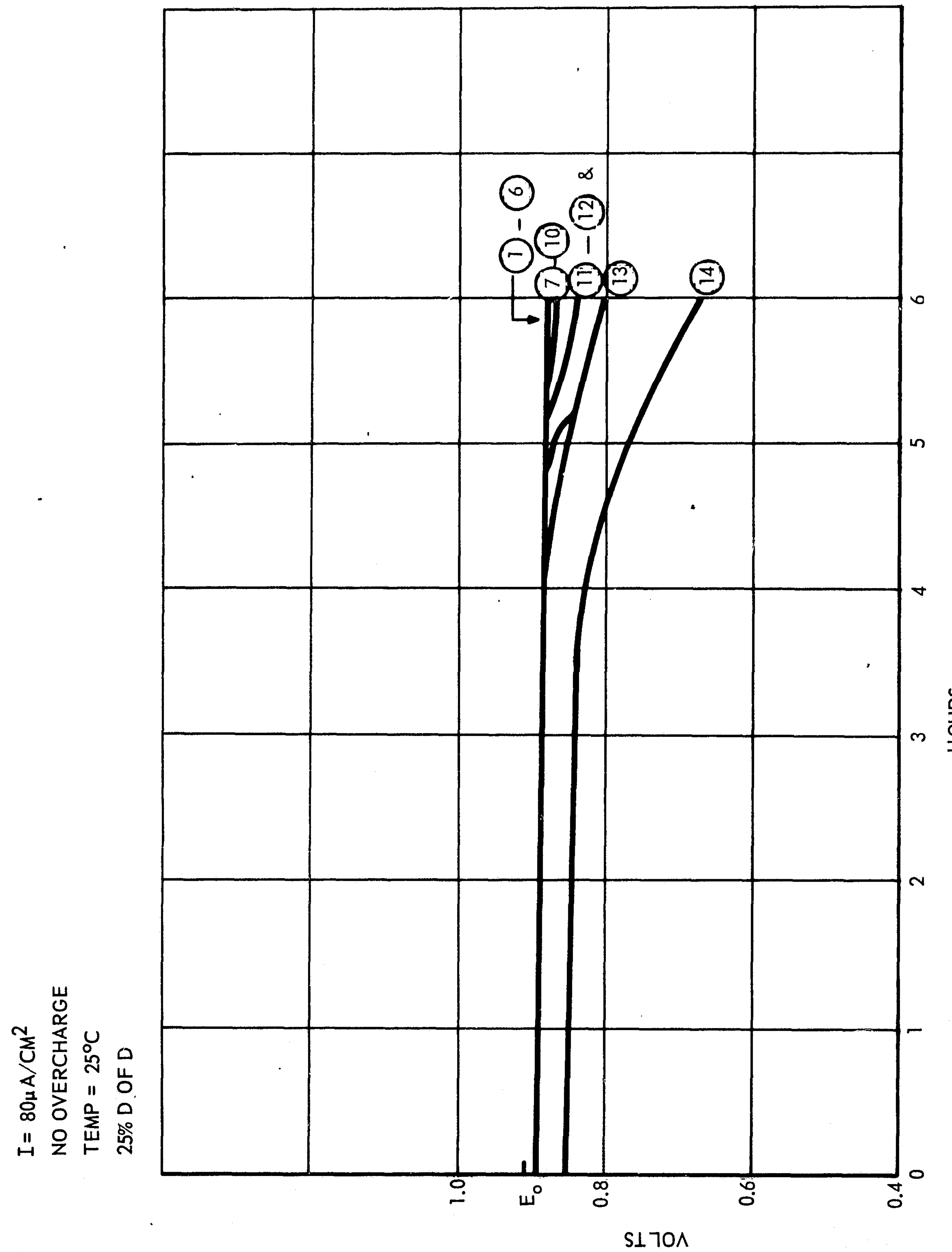

Figure 12. Performance Curves for Cell No. 48-80

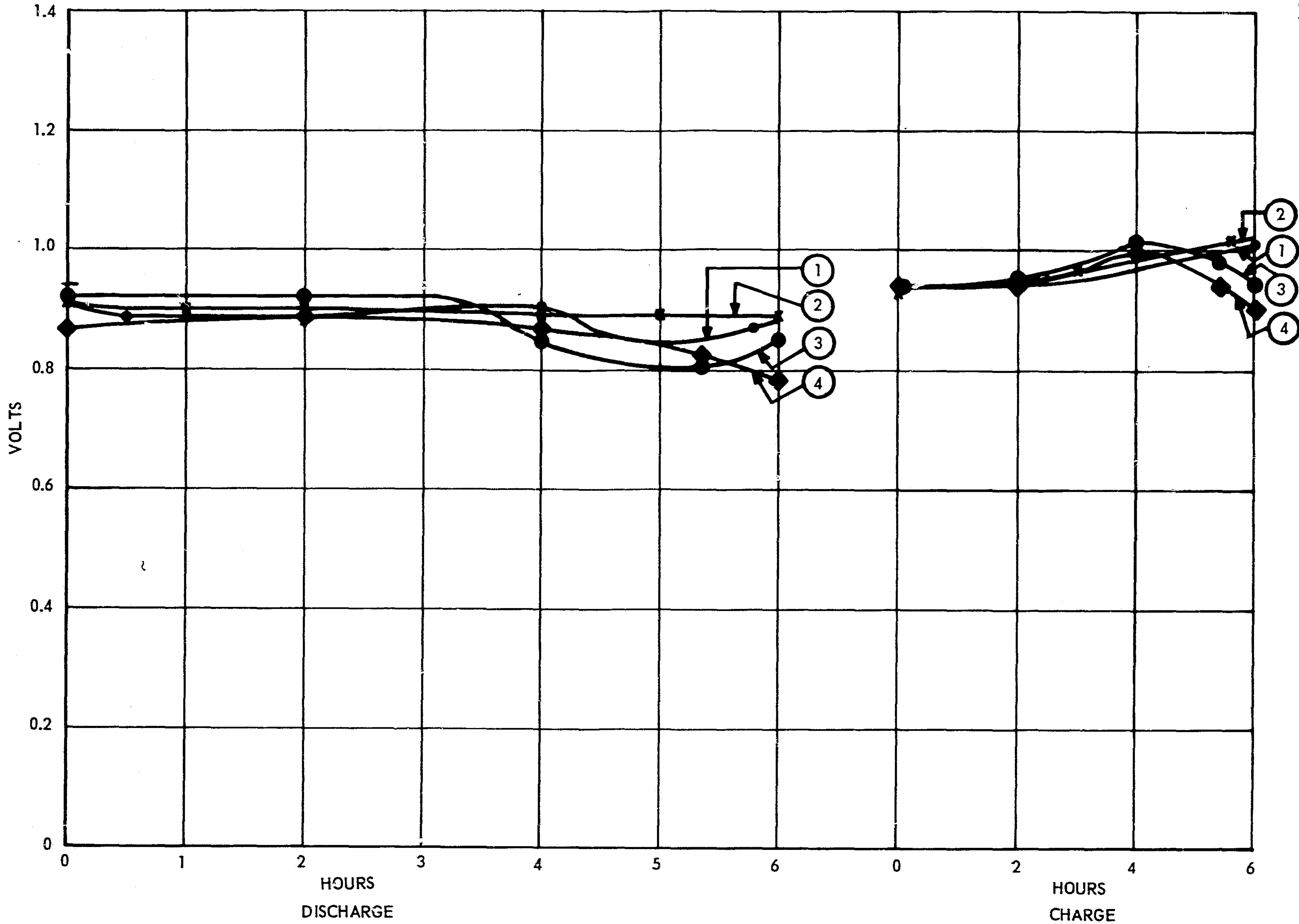

Figure 13. Performance Curves for Cell No. 48-65 (Sheet 1 of 2)

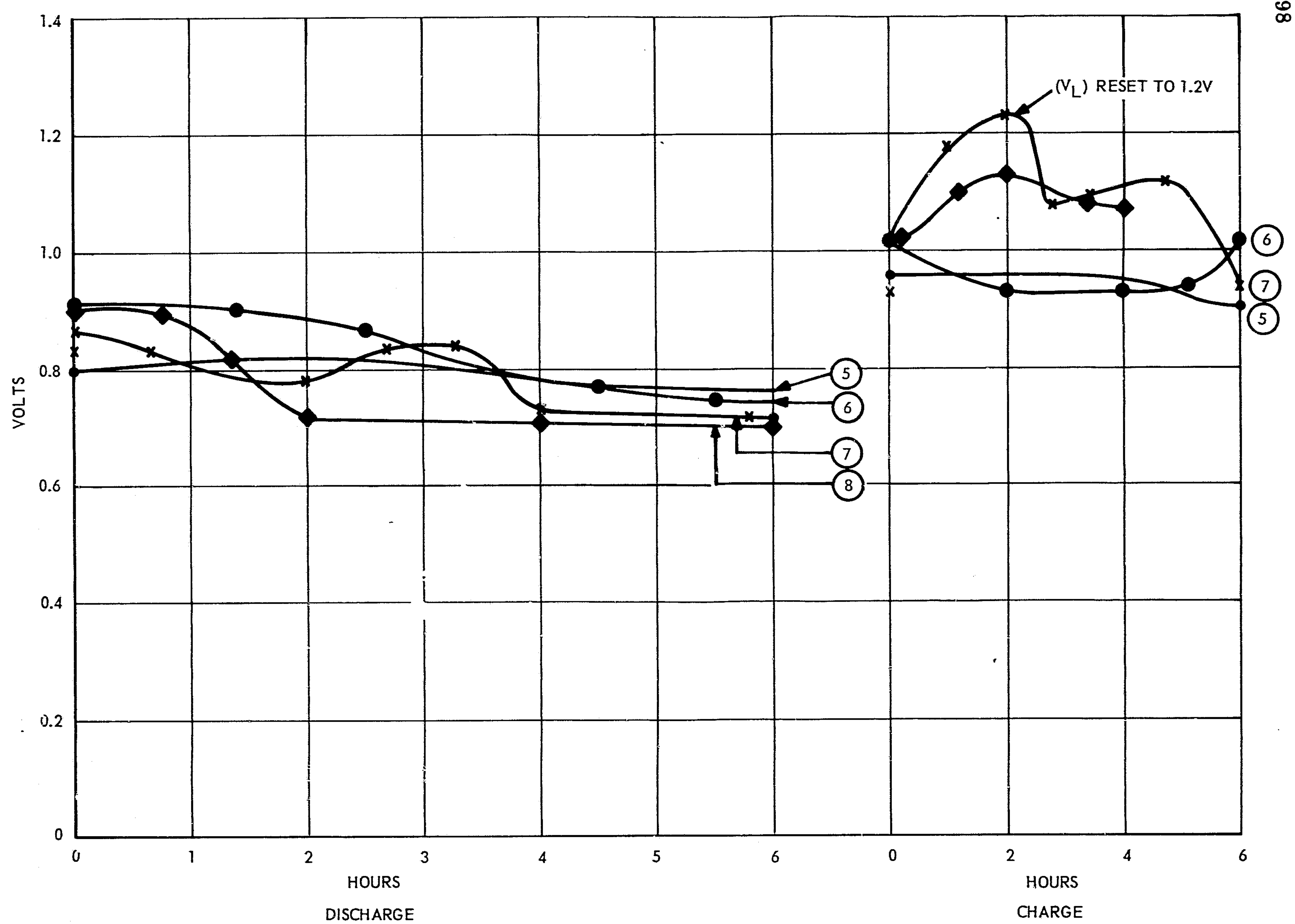

Figure 13. Performance Curves for Cell No. 48-65 (Sheet 2 of 2)

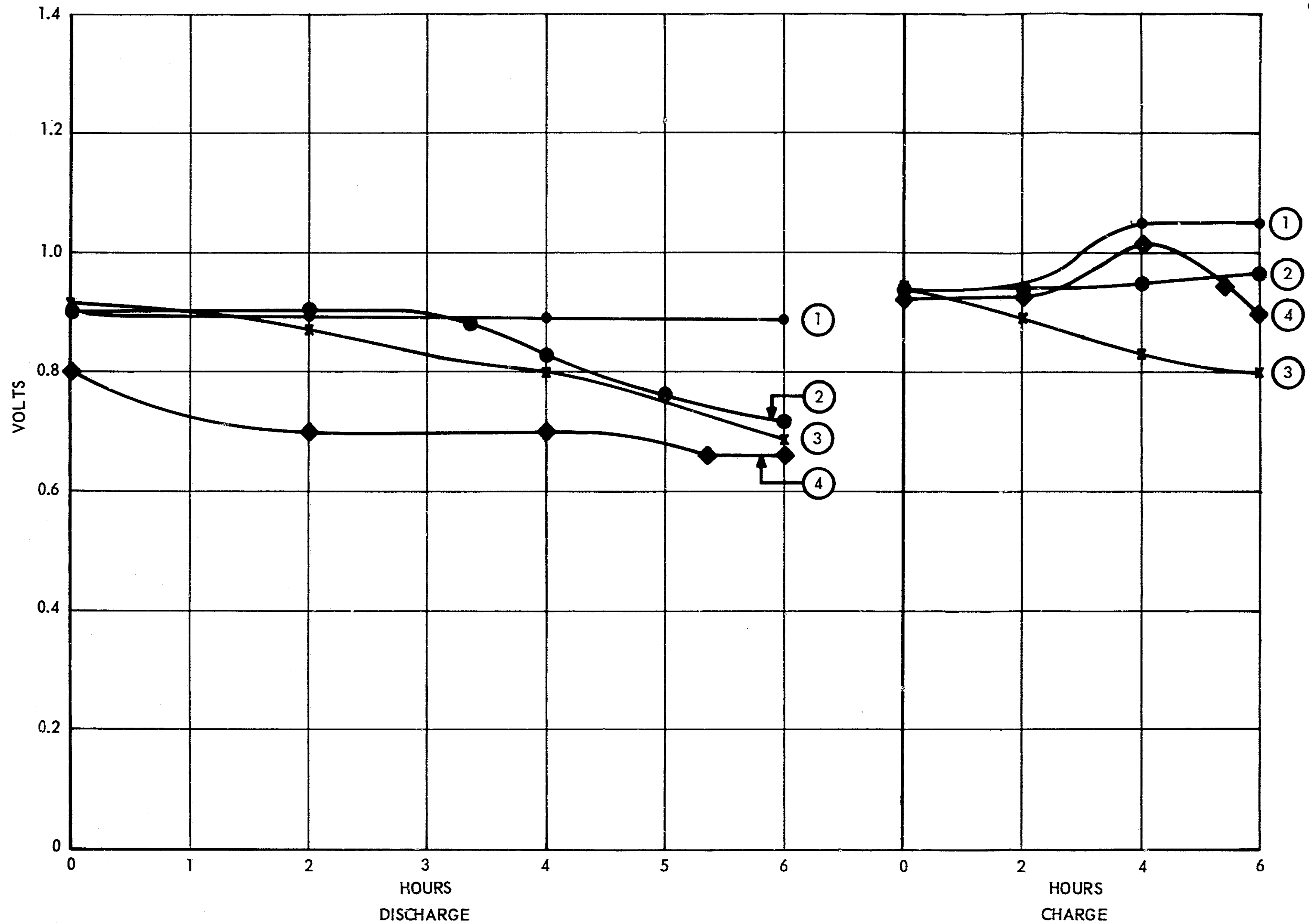

Figure 14. Performance Curves for Cell No. 48-66 (Sheet 1 of 2)

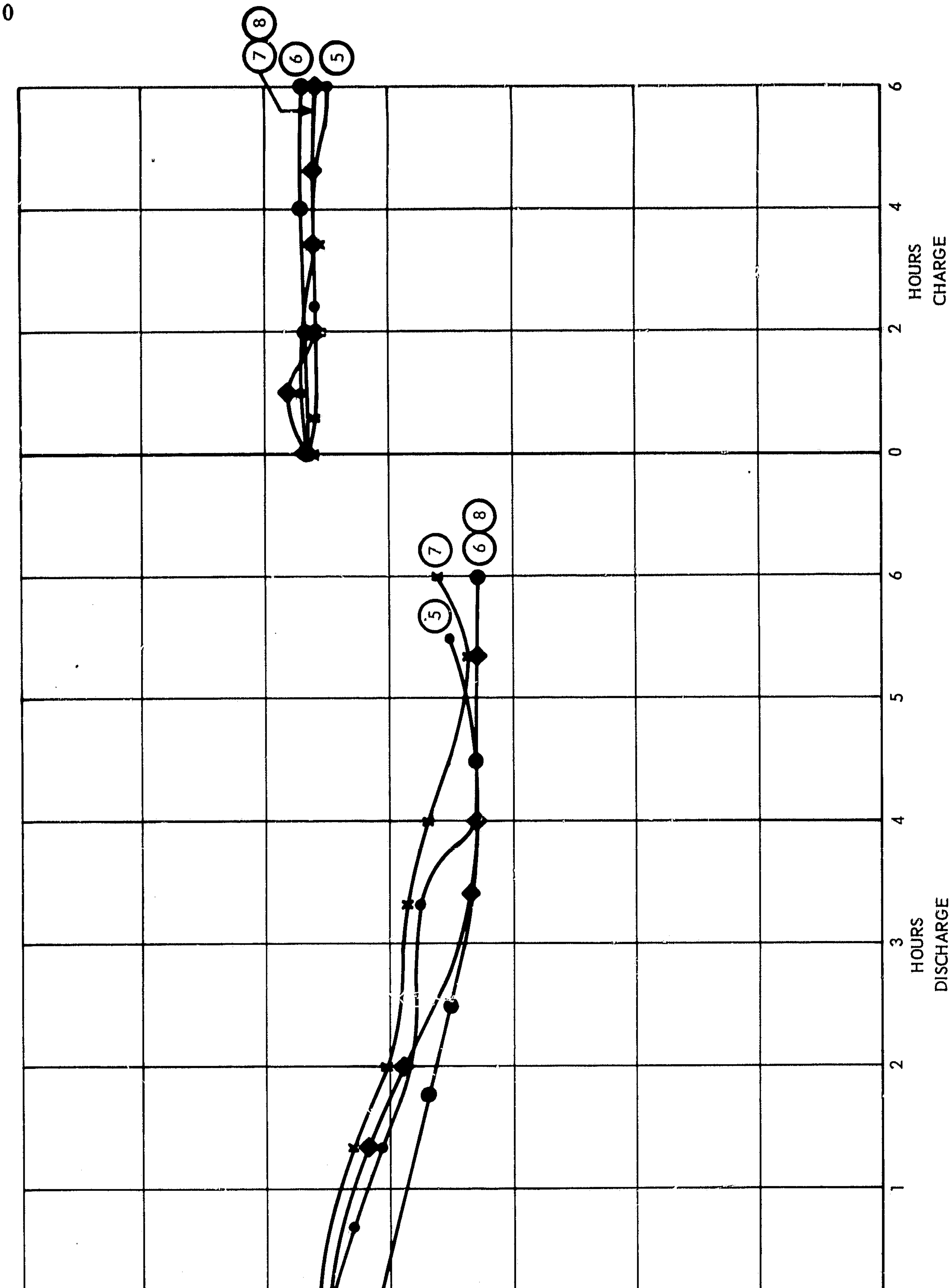

Figure 14. Performance Curves for Cell No. 48-66 (Sheet 2 of 2)

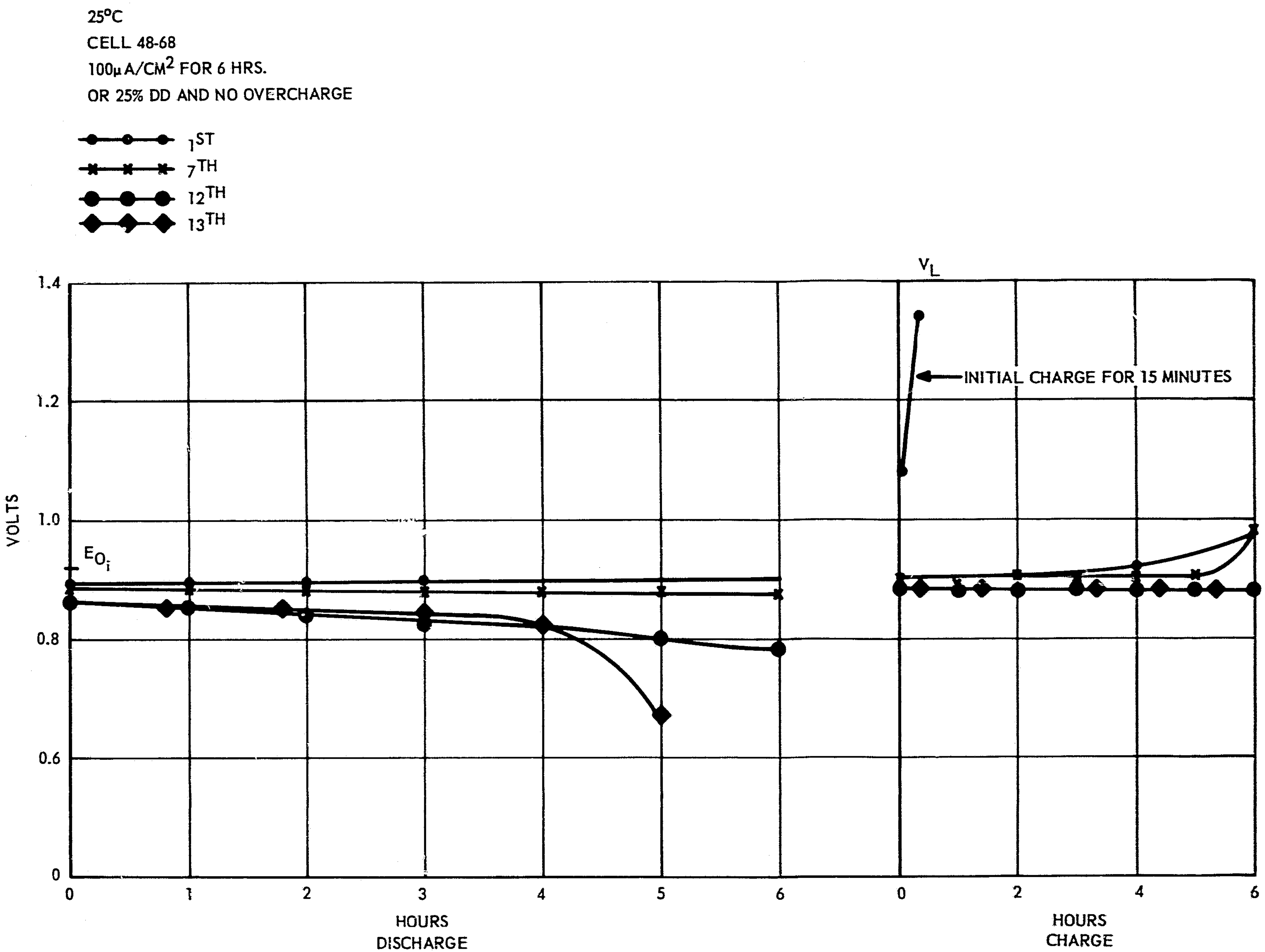

Figure 15. Performance Curves for Cell No. 48-68

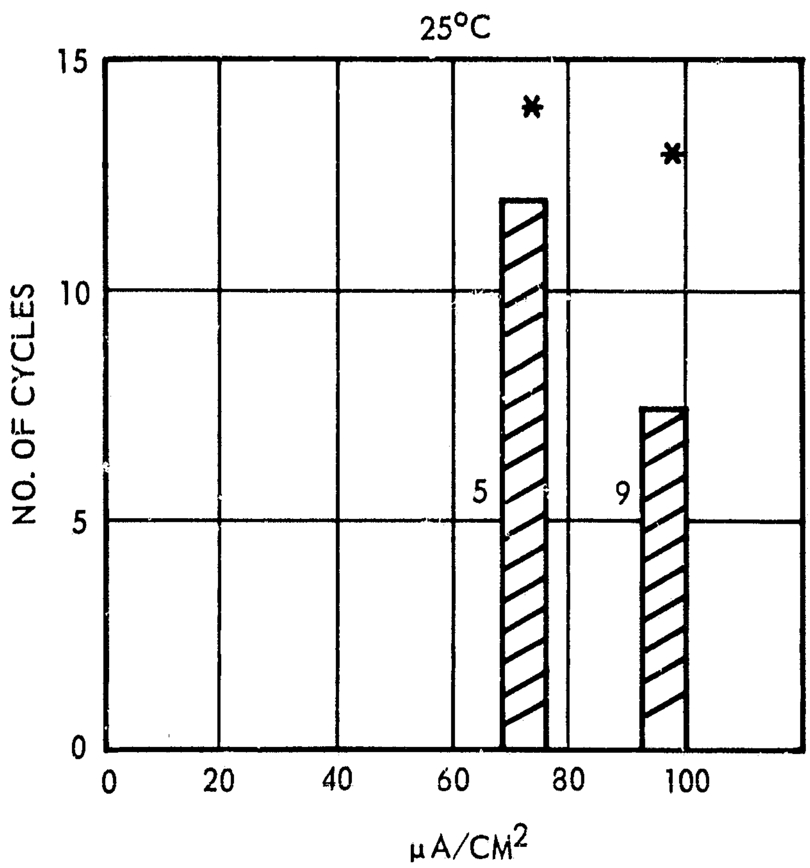

NOTE: * MEANS MAXIMUM
NO. OF CYCLES
NUMBER TO THE LEFT
MEANS NO. OF BATTERIES
USED FOR THE AVERAGE.

Figure 16. Average No. of Cycles for Various Discharge Rates

rechargeability at 0°C. Generally, the internal resistance of the cell increased 2.5 to 3 times as it was cooled from 25°C to 0°C. Frequently, it was observed that the cell resistance was higher than this until it had discharged for a few minutes and in some cases had been recycled a few times. Therefore, some conditioning of this type may be required before the cell is ready for operation.

The cell performance at 0°C is summarized in Table 3. Data are presented for four current density ranges (62-80, 93-100, 132-155, 200 $\mu A/cm^2$), three discharge depths (9-15, 25, 40-50%) and two overcharge ranges (8-13, 25%). The actual discharge capacity was again assumed to be 15 mAh and the values given in Table 3 are calculated as per cent of actual capacity (AC). Figures 17-23 are representative of the cell performance at the rates specified and are summarized as follows:

Cell No.	I/cm^2	%DD	%OC	No. of Cycles
48-111	80	40	10	8
115	80	10	25	11
48-104	93	15	13	20
107	100	25	9	21
48-113	132	15	25	28
98	155	25	12	21
48-99	200	50	8	9

Cell no. 48-85 was recharged the maximum number of cycles, 35, without overcharge and cell no. 48-113 was recharged the

TABLE 3

Cycling Results at 0°C With Overcharge

Cell No.	Eo_i volts	I µA	I/Area µA/cm²	Discharge mAh	Discharge %(AC)	Charge %OC	No. of Cycles
48-82	0.948	400(Av.g.)	62	2.4	16	-	16
48-83	0.910	325-410	62	2.4	16	-	17
48-84	0.918	400	62	2.4	16	-	22-24
48-85	0.908	380-400	62	2.4	16	-	35
48-90	0.950	1,000	155	3.75	25	12	8
48-91	0.892	1,000	155	3.75	25	12	14
48-92	0.966	1,000	155	3.75	25	12	8
48-98	0.970	1,000	155	3.75	25	12	21
48-93	0.972	625-700	108	2.65	17.5	12	14
48-95	0.974	500-700	108	2.65	17.5	12	7
48-96	0.972	2,000	310	7.50	50	13	2-6
48-97	0.972	2,000	310	7.50	50	13	2-6
48-100	0.940	2,000	310	7.50	50	13	6
48-99	0.942	1,300	200	7.50	50	8	9
48-101	0.980	1,300	200	7.50	50	8	9
48-102	0.970	1,300	200	7.50	50	8	10
48-104	0.968	600	93	2.25	15	13	20
48-105	0.980	600	93	2.25	15	13	20
48-106	0.964	600	93	2.25	15	13	8
48-107	0.988	650	100	3.75	25	9	21
48-108	0.978	650	100	3.75	25	9	16
48-109	0.984	650	100	3.75	25	9	12
48-110	0.984	650	100	3.75	25	9	15
48-111	0.984	520	80	6	40	10	8
48-112	0.974	520	80	6	40	10	11
48-113	0.984	[illegible]50	132	2.25	15	25	28
48-114	0.958	850	132	2.25	15	25	20
48-115	0.944	500	78	1.33	9	25	11
48-116	0.966	800	125	2.12	14	26	6
48-118	0.942	800	125	2.25	15	25	7
		1,400	225	3.75	25	25	2
51-1	0.996	600	93	2.25	15	13	7
B-1	0.944	1,000	[illegible]20	3.75	-	13	10
B-2	0.9[illegible]4	5,000	100	29	-	9	3
		2,000	40	11.5	-	9	8

%AC - % Actual Capacity (15 mAh)

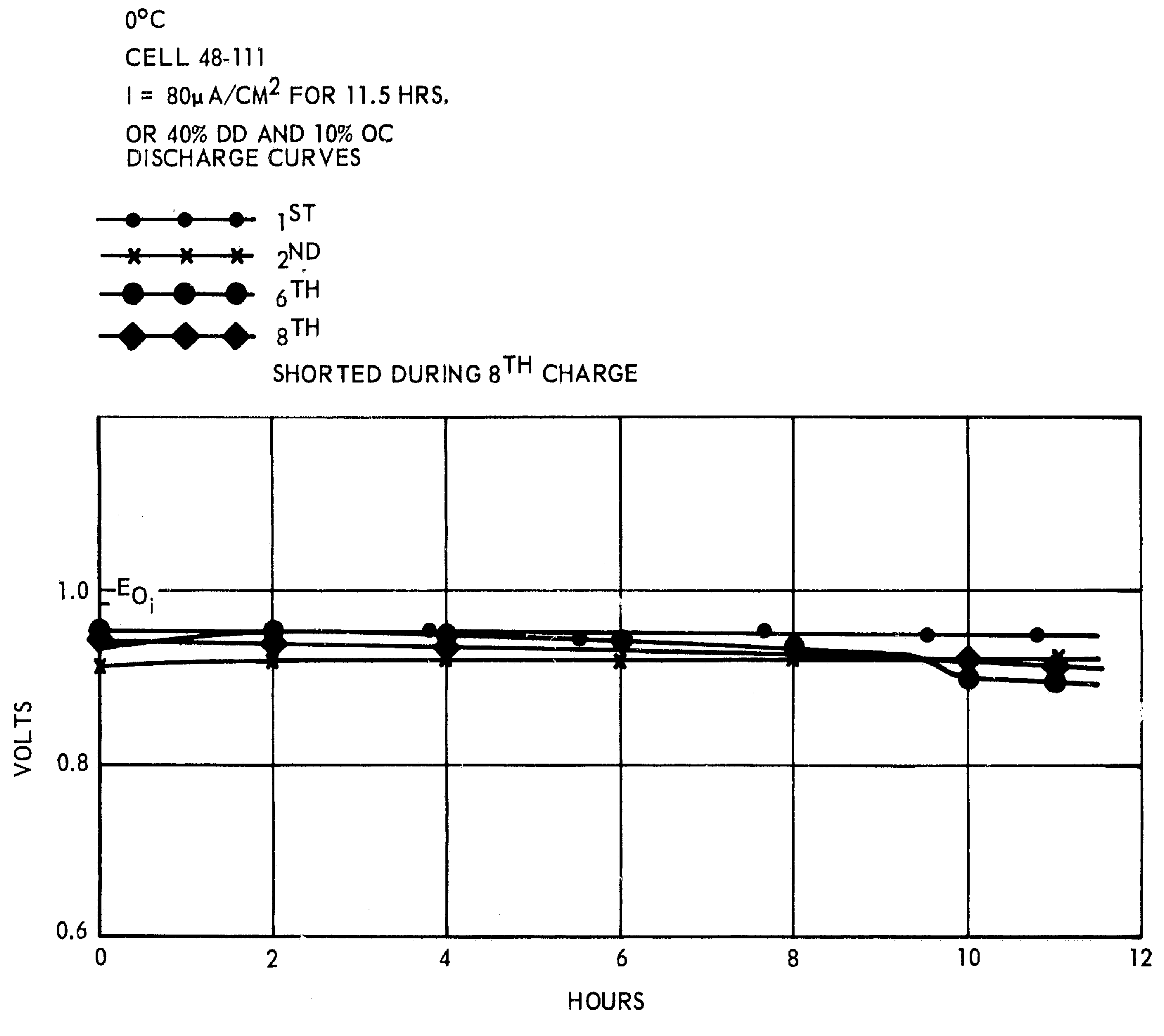

Figure 17. Performance Curves for Cell No. 48-111 (Sheet 1 of 2)

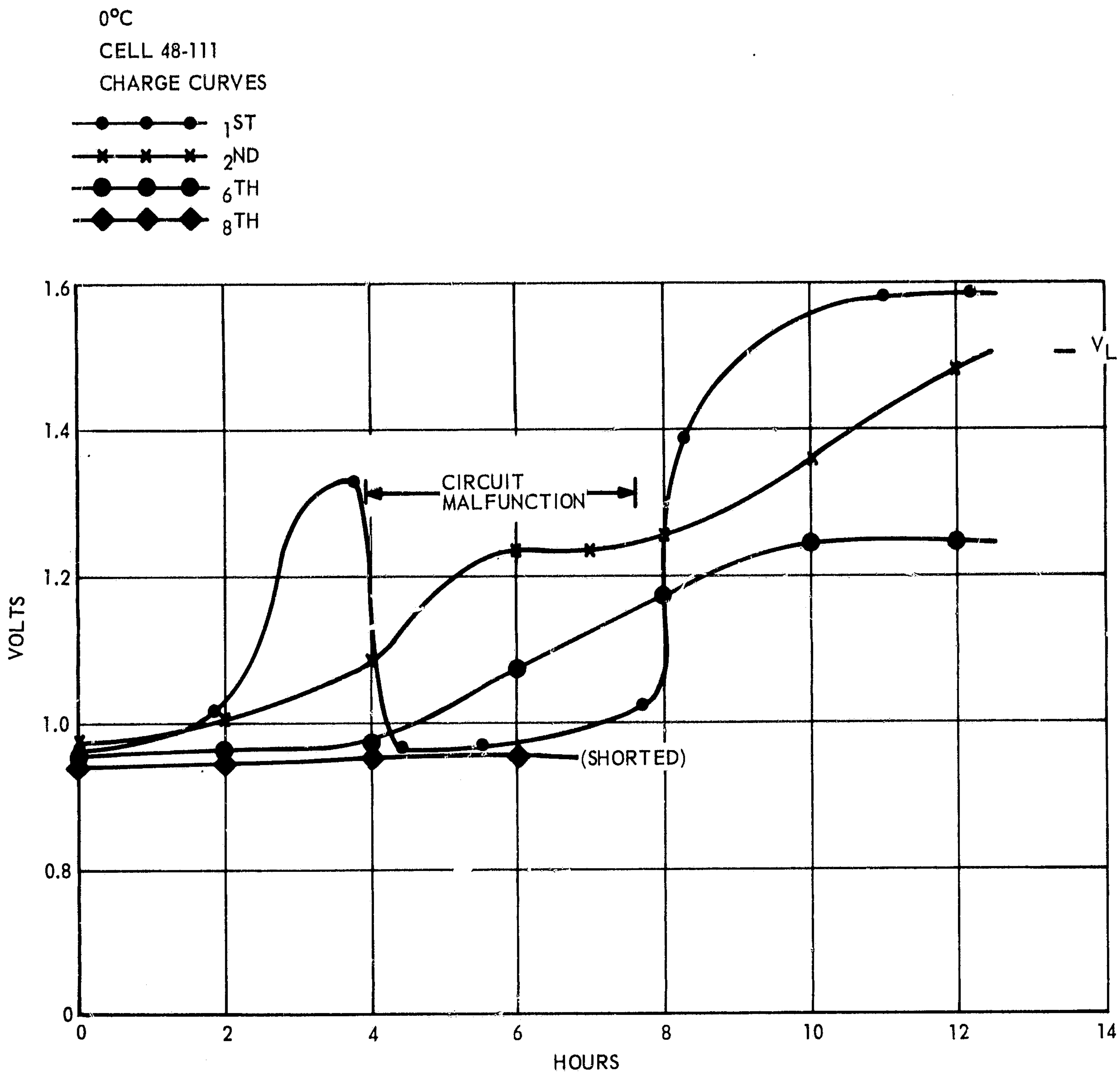

Figure 17. Performance Curves for Cell No. 48-111 (Sheet 2 of 2)

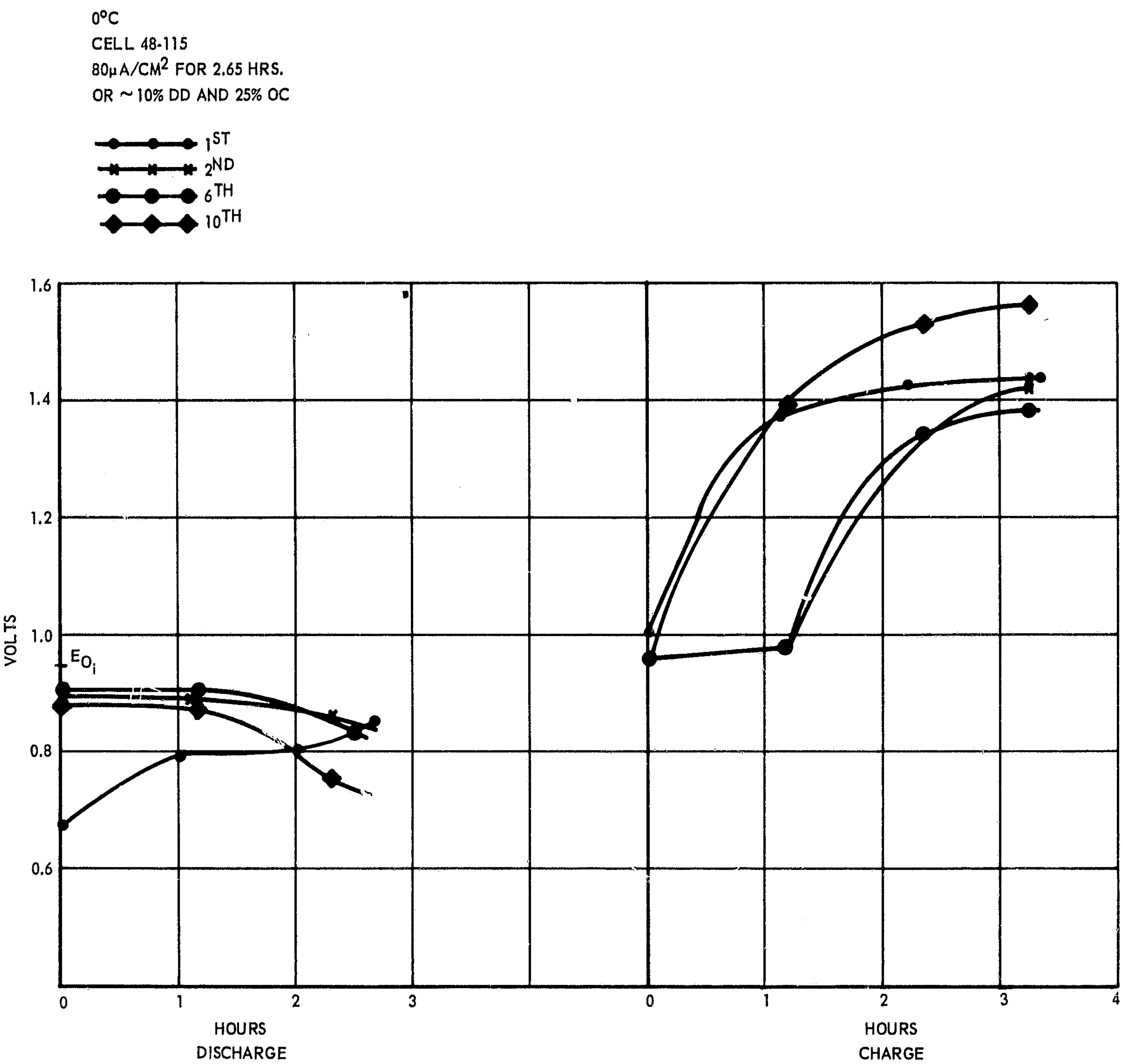

Figure 18. Performance Curves for Cell No. 48-115

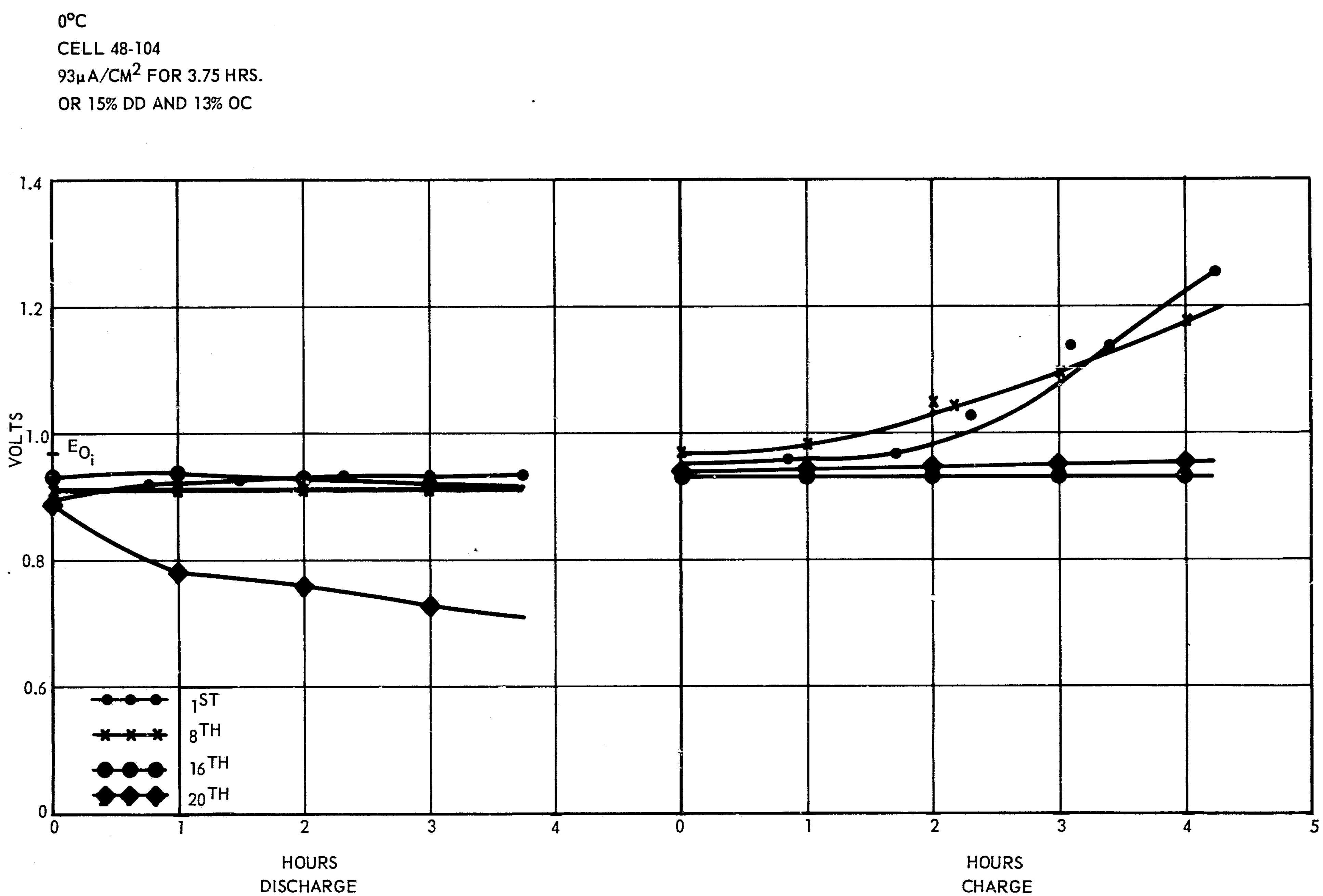

Figure 19. Performance Curves for Cell No. 48-104

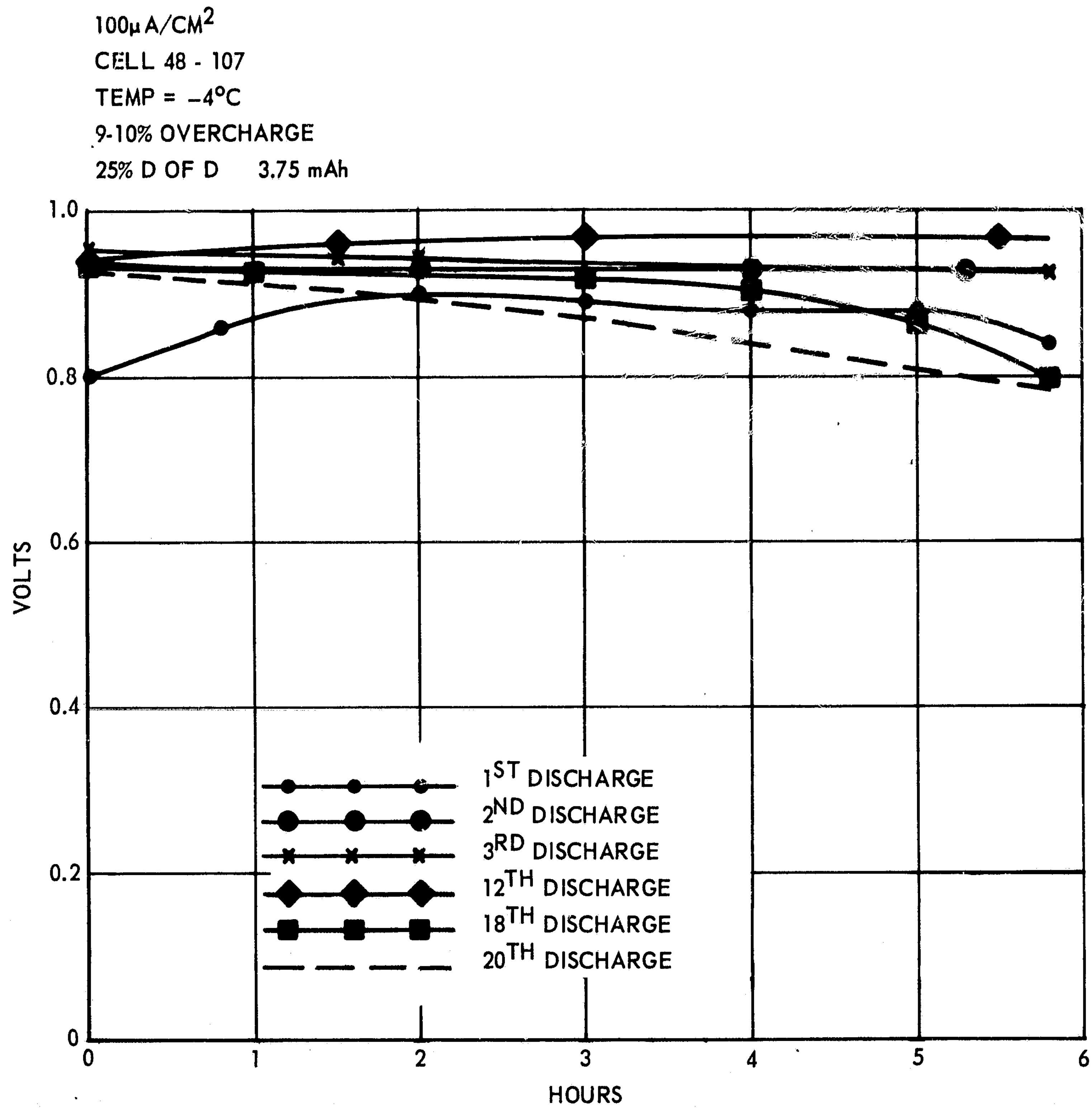

Figure 20. Performance Curves for Cell No. 48-107 (Sheet 1 of 2)

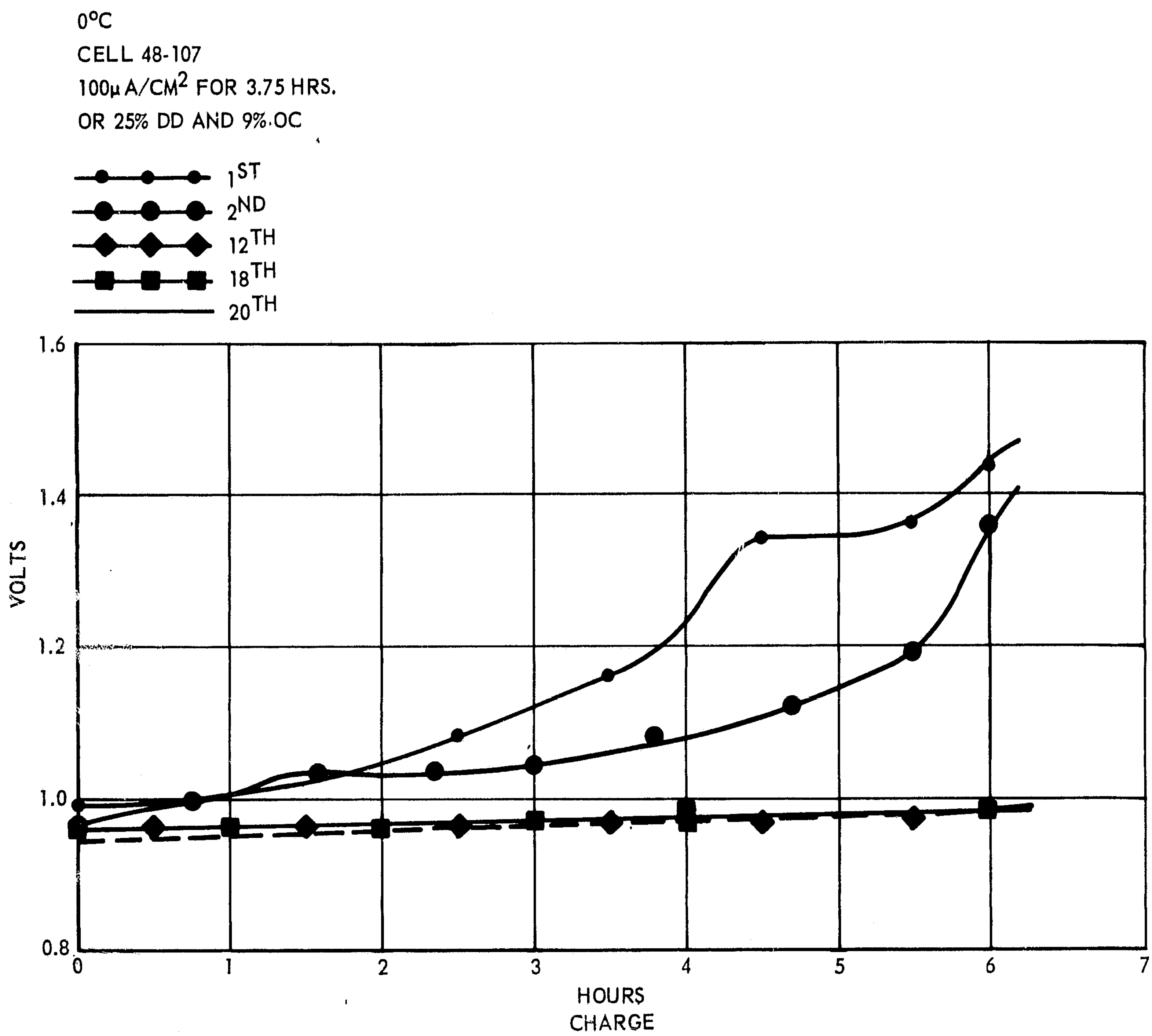

Figure 20. Performance Curves for Cell No. 48-107 (Sheet 2 of 2)

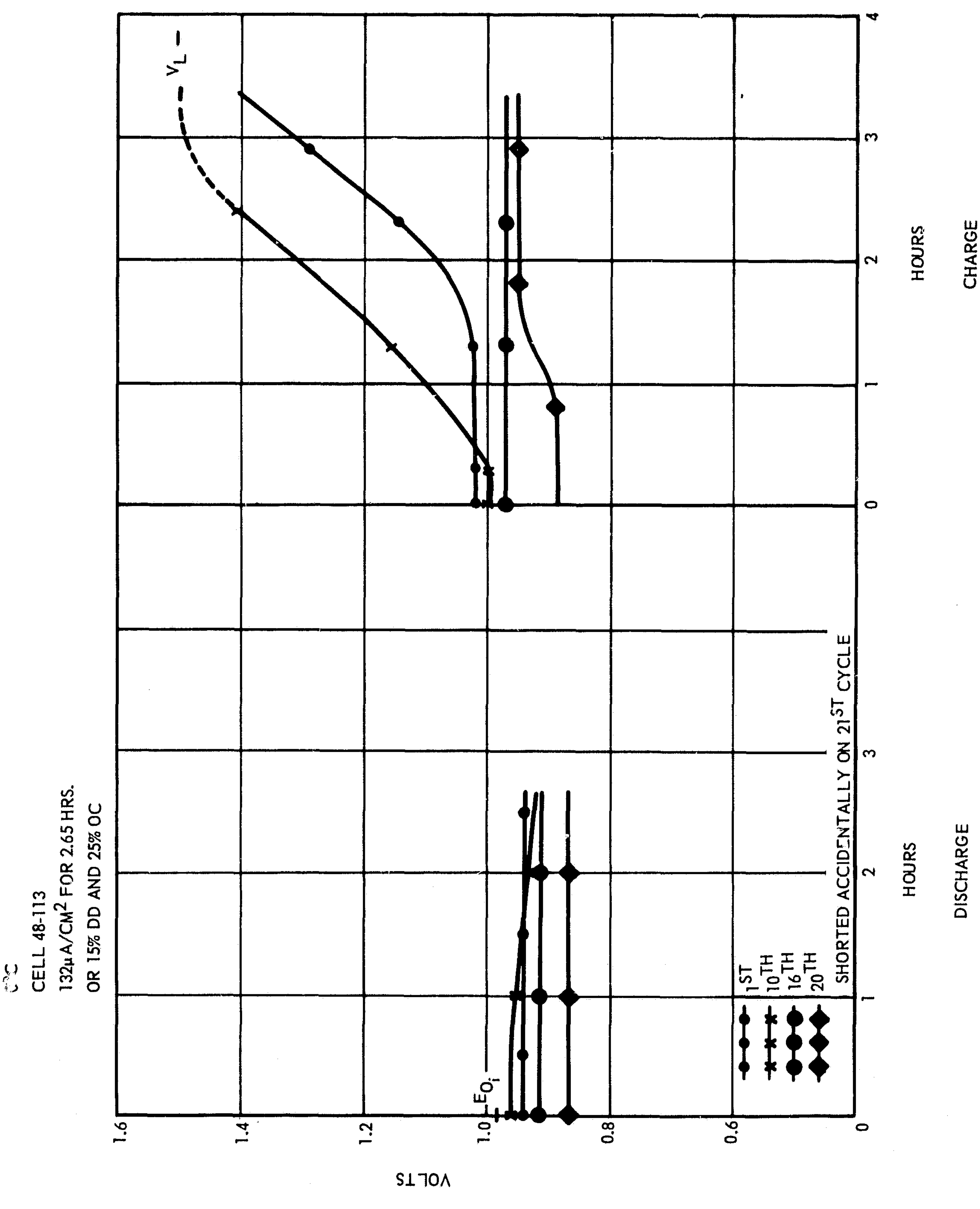

Figure 21. Performance Curves for Cell No. 48-113

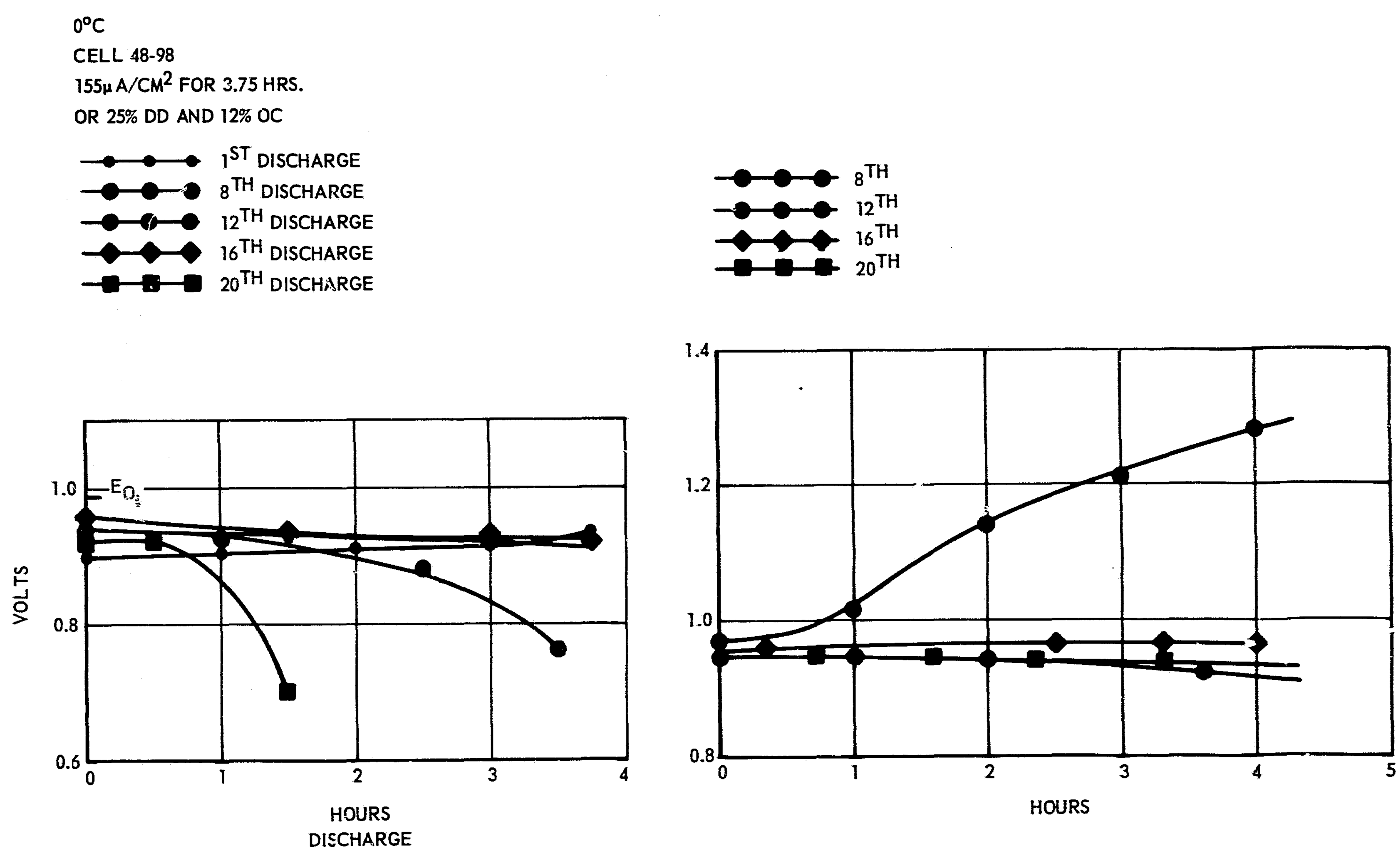

Figure 22. Performance Curves for Cell No. 48-98

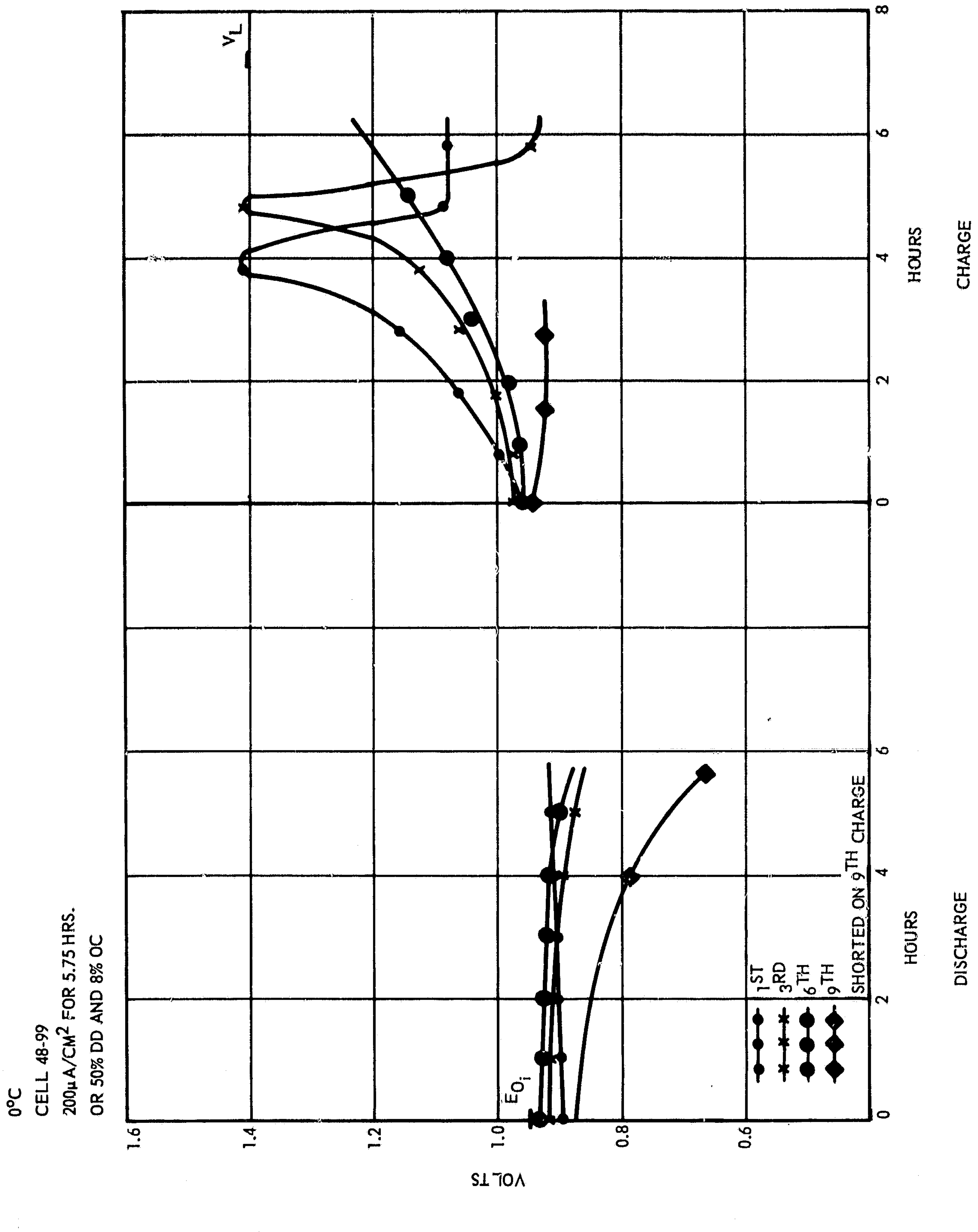

Figure 23. Performance Curves for Cell No. 48-99

maximum number of cycles, 28, with an overcharge. At the higher current rates the cells frequently reached a high charging voltage (1.4 - 1.6 volts) during the early cycles. Therefore, the voltage limit was set at its maximum of approximately 1.5 volts. A few times this voltage limit was exceeded and the charging current reduced thus reducing the per cent of overcharge for that particular cycle.

Figure 24 illustrates the average number of cycles for several current densities and for no overcharge, 8-13% overcharge, and 25% overcharge.

One can conclude that the Ag-Zn electrochemical system is definitely rechargeable and capable of producing usable current densities at 0°C. A large number of the batteries failed by internal shorting and thus the cycle life may be extended greatly if this can be prevented by improved fabrication methods and modified cell structure.

Near the end of the program two large batteries were fabricated and tested and designated B-1 and B-2. Each had an area of 50 cm^2 and theoretical capacities of 50 mAh (1 mAh/cm^2) and 200 mAh (4 mAh/cm^2) respectively. The cells were fabricated by the procedure given in Section 1. Figure 25 is the V-I curve for B-1 and Figure 26 the first discharge at 5 mAh or 100 $\mu A/cm^2$ at 0°C for 7.5 mAh. The initial internal resistance was 5 ohms. Because of a circuit failure, B-1 was shorted externally for several seconds and the additional data was taken at a 1 mA discharge rate.

B0272

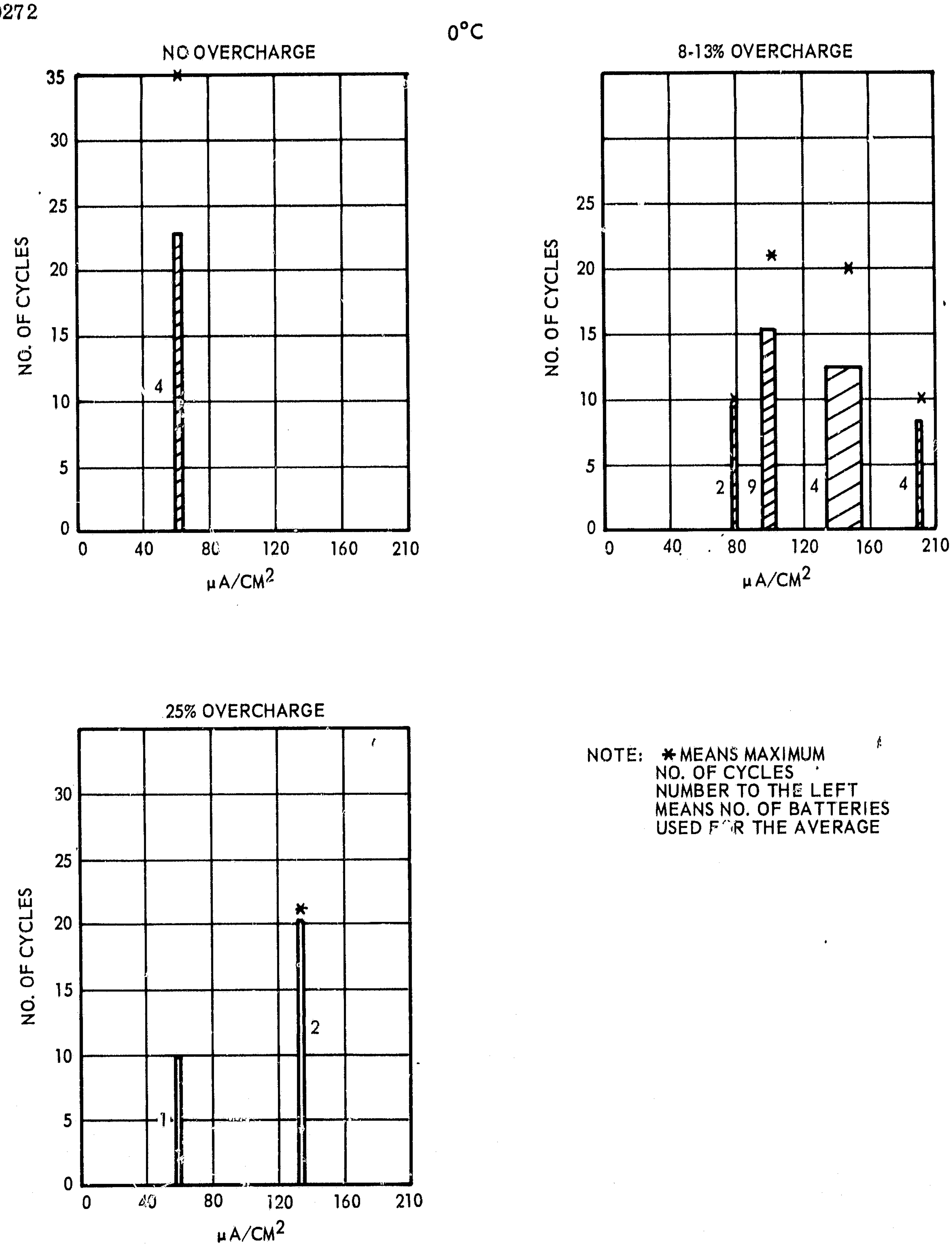

Figure 24. Average No. of Cycles for Various Discharge Rates

B0324

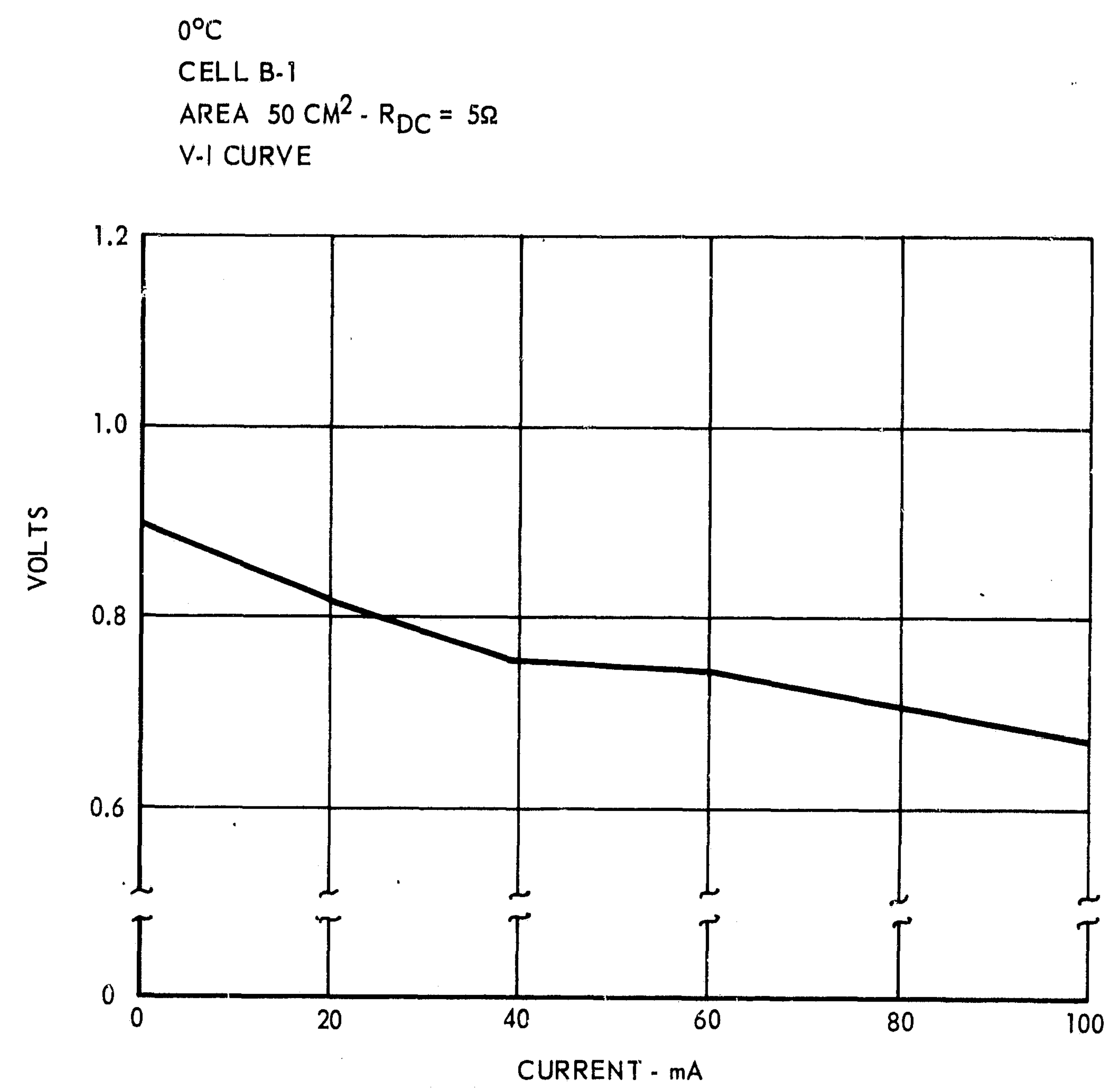

Figure 25. V-I Curve for Cell No. B-1.

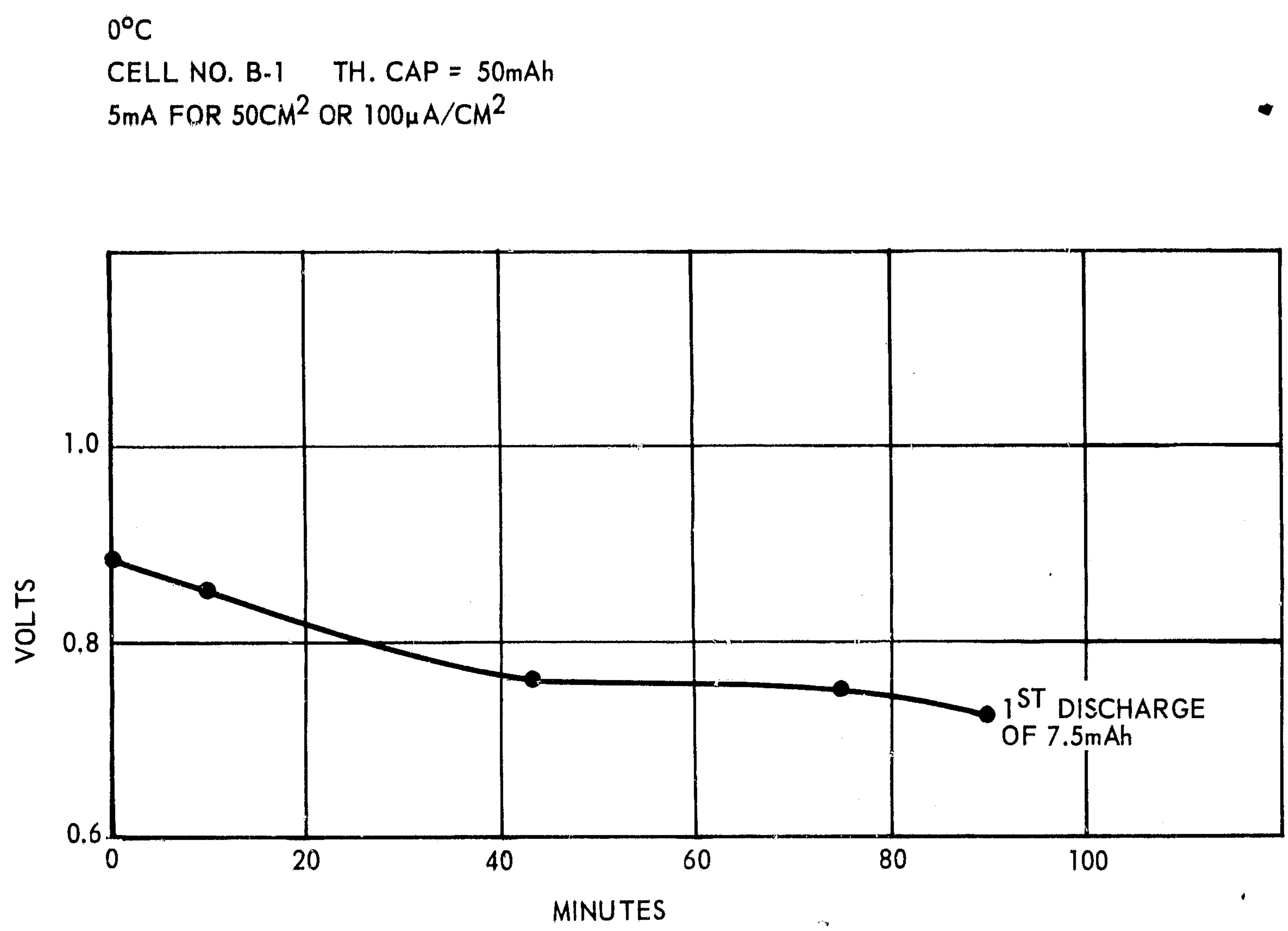

Figure 26. First Discharge of Cell No. B-1

Cell B-2 was discharged initially at 5 mA or $100 \mu A/cm^2$ and after the third cycle the discharge was reduced to 2 mA or $40 \mu A/cm^2$ for the remaining 8 cycles. Figure 27 and Figures 28A and B show the performance of B-2. The initial internal resistance was 10 ohms. The principal difficulty in fabricating these large cells was achieving a uniform distribution of the electrolyte over the 50 cm^2 by dipping. New techniques and better electrolyte binders should prevent this problem in the future. The Ag of cell B-2 was converted at a rate of 4 mAh/cm^2 for 1 hour in order to compare its performance with the smaller cells (6.45 cm^2 area). The initial discharge of B-2 at $100 \mu A/cm^2$ illustrates the feasibility of scaling up the cell nearly 8 times in area.

6.3. Shelf Life

Cells were periodically removed from the fabrication assembly, placed in a pressure clamp and left at room temperature. Many of the cells shorted before the end of the contract period for reasons which we expect to establish in the near future. Those cells, fabricated in the early part of the program, did not have the additional tape enclosure and perhaps moisture from highly humid air may have caused the shorting. It may also be possible that initial excess moisture in the cells caused significant electronic conductivity.

Data for 10 batteries were recorded and will be reported when the failure mechanism is well established.

B0325

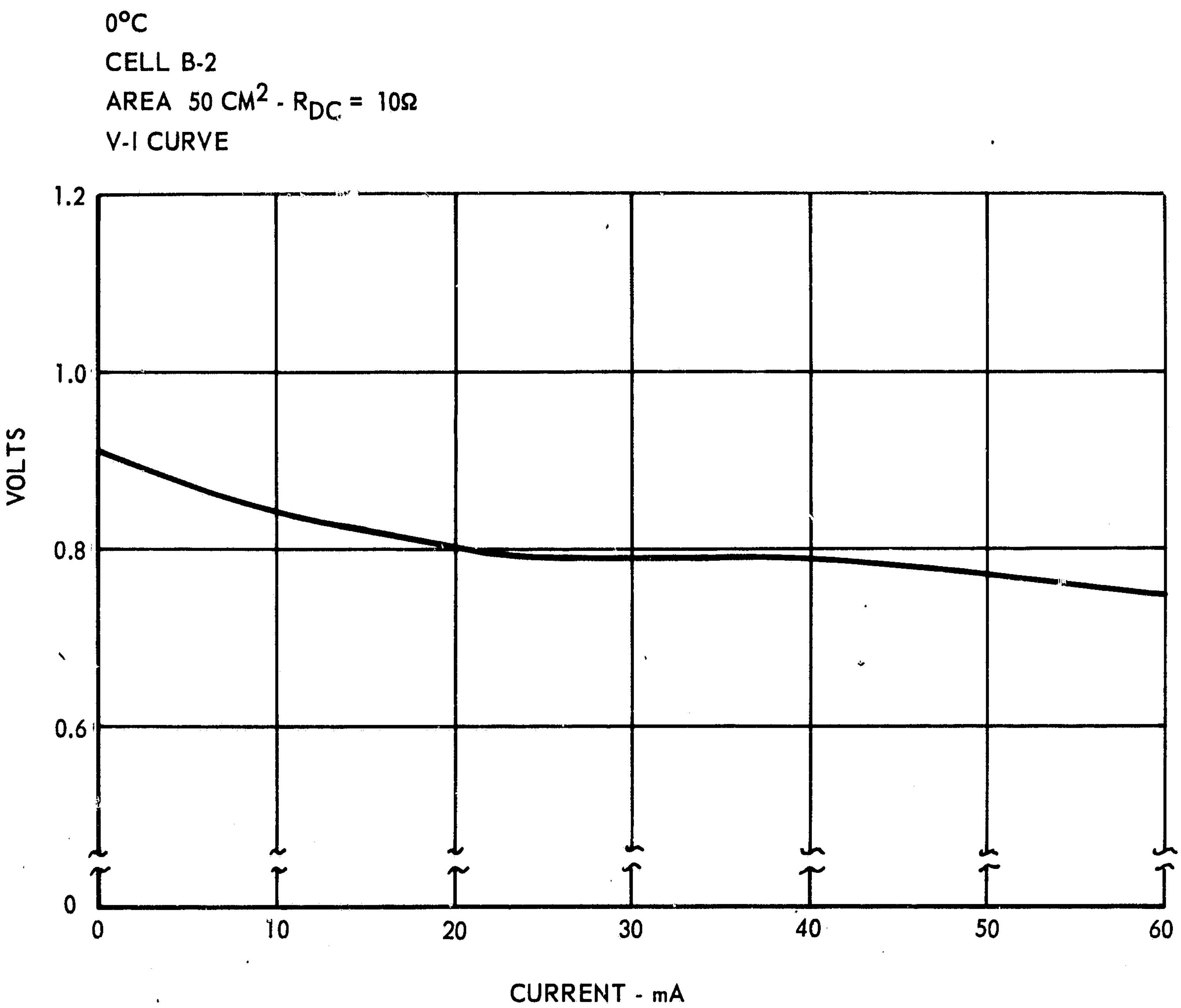

Figure 27. V-I Curve for Cell No. B-2

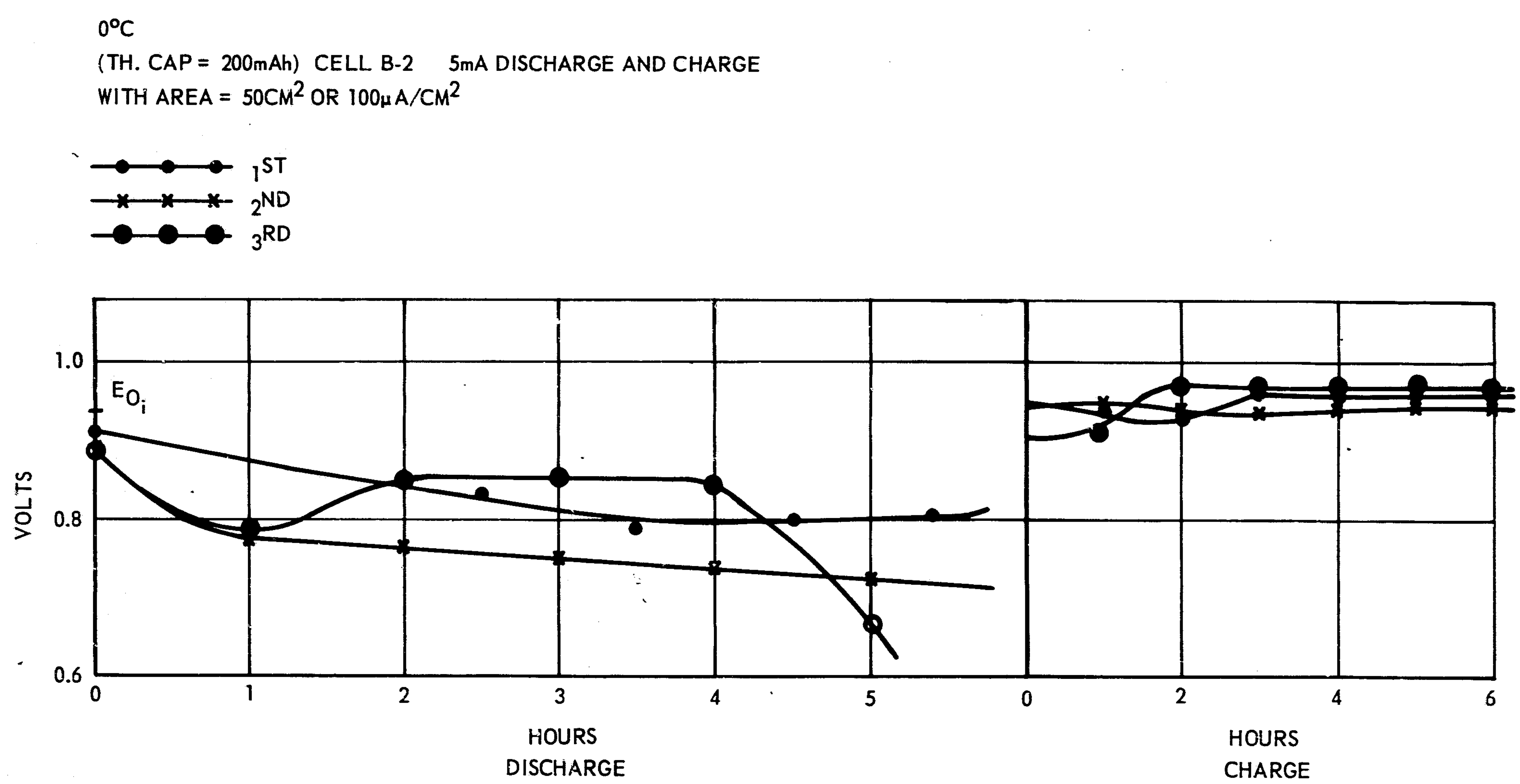

NOTE: 3^{RD} CHARGE AT 2mA

Figure 28. Performance Curves for Cell No. B-2 (Sheet 1 of 2)

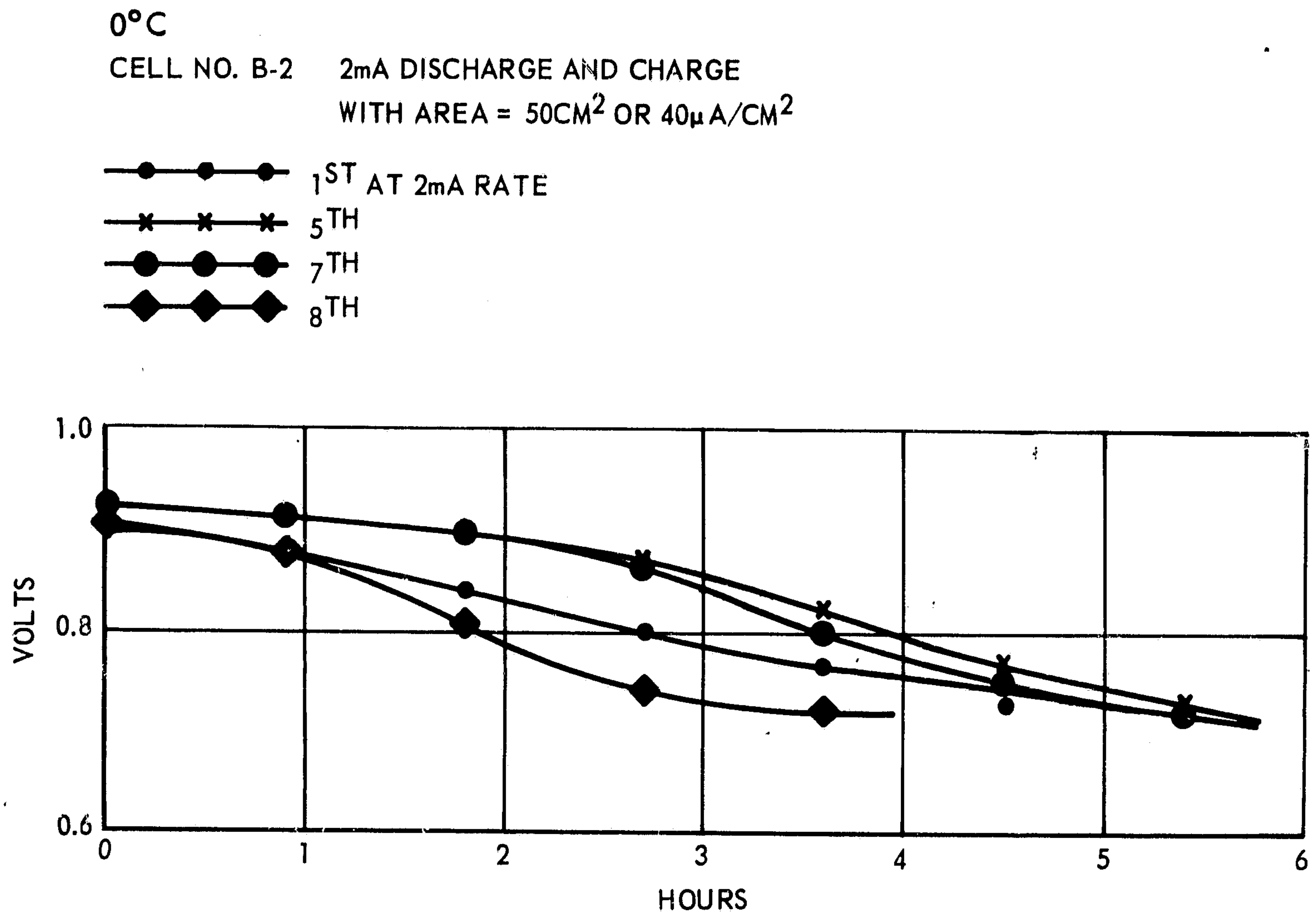

Figure 28. Performance Curves for Cell No. B-2 (Sheet 2 of 2)

7. CONCLUSIONS AND RECOMMENDATIONS

The results of this program have established the feasibility of the Ag-Zn solid electrolyte system as a rechargeable electrochemical cell at 0°C. The number of cycles can be increased by overcharge as long as the charging potential does not become so great that it will short the cell. It was observed that 1.4 - 1.6 volts was the maximum permissible charging voltage.

One principal problem was cell polarization at current densities exceeding $125 \mu A/cm^2$ although current densities of $25\ mA/cm^2$ were possible before the cell voltage dropped to 0.72 volts (Figure 4).

Since this is a new battery system and relatively little is known of its real capabilities, a number of recommendations for future investigations and improvements are given below:

1. Increase the per cent of utilization of the active materials in order to increase the watt hours/lb for the system.
2. Investigate new electrolyte binding and separating materials.
3. Study the chemical reactions occuring during discharge and charge.
4. Study of the failure mechanisms.

5. Investigate methods of reducing the cathodic polarization.
6. Measure the electronic conductivity of the electrolyte.
7. Improve the packaging techniques to assure against permeability of moisture and to reduce battery weight.
8. Investigate the ionic transport properties of the electrolyte and the AgCl.